



國立臺灣大學理學院氣候變遷與永續發展碩士學位學程

碩士論文

International Master Degree Program in Climate Change and Sustainable  
Development

College of Science

National Taiwan University

Master Thesis

探討棲蘭雲霧森林在低土壤濕度期間的植物生長與降水變化  
的關係

Unique Responses of Vegetation During the Low Soil Water  
Periods under the Change of Precipitation in Chi-Lan Montane  
Cloud Forest

林思穎

Szu-Ying Lin

指導教授：羅敏輝 博士、莊振義 博士

Advisor: Min-Hui Lo, Ph.D. & Jehn-Yih Juang, Ph.D.

中華民國 111 年 12 月

Dec. 2022

## 誌謝

謝謝羅老師耐心的指導，讓我學習了如何去思考問題，並在思考的過程中慢慢摸索整理重點的方法。謝謝棲蘭組的鎔與學姊、譯心學姊、子瑩和璟宏，帶我認識棲蘭這個優雅的森林，在風雨無阻下，一起維護通量塔、樹液流和開放地的測站。謝謝莊振義老師與黃倬英老師提供的通量塔資料，透過對棲蘭 meeting 了解很多不通面向的知識。謝謝小松光老師與謝宜桓老師在每次 seminar 結束之後願意空出時間與我討論，並獲得很多建議。也謝謝實驗室的成員、IPCS 的成員在研究上和課業上的幫助。最後謝謝我的家人、隔壁實驗室的宜臻、社團的成員們，在這兩年給予的支持和鼓勵。

## 中文摘要



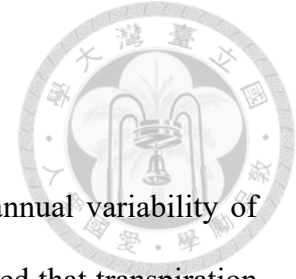
降雨是熱帶森林中影響植物生長年際變化的重要因子之一。舉例來說，年降雨量大於 2000mm/yr 的地區在乾季具有充足的可用水，使植物在乾季更有效率地進行光合作用。相比之下，年降雨量小於這個門檻值的地區，則受到水分的限制。前人研究發現，雲霧森林具有比一般森林更充沛的水分來源，但蒸散作用和植被初級生產量卻低於一般熱帶森林，這之間的差異可能與能量的限制有關係。

本研究比較了台灣的兩個森林地區，棲蘭（雲霧森林）和蓮華池（典型一般森林），並分析其通量塔的降水資料與衛星觀測的植生指數，觀察兩者在土壤較乾的季節下是否具有相關性。觀測資料的結果顯示，在較乾燥的環境中（1月至4月），兩個森林對水分的需求表現不同。前一年年底的累積降水，藉由傳送至土壤再供給至植物，使蓮華池地區在隔年春季的光合作用更有效率；而棲蘭雲霧森林的植生指標在降水變化下則沒有顯著相關。

我們進一步利用陸地模式，在不變動其他天氣因子的理想化條件下，對降水的量值進行了測試，並分析所模擬的蒸散和光合作用變化。我們發現當地微氣候（降水、溫度等）在水文循環過程比地表特性和植物種類更影響光合作用的進行，同時在典型森林的降雨與植被的生長能力之間存在非線性的關係，其來自於土壤水分變化和植物大氣之間的蒸氣壓差。相反的，棲蘭由於土壤含水量相對偏高，植物生長狀態在乾季較不受影響，這也是雲霧森林獨有的特徵，在未來氣候變遷，乾季越乾以及水分減少的狀況下，有機會繼續維持植物的生長，並在碳吸收過程中扮演著相當重要的角色。

關鍵字：雲霧森林、降水、植生指數、光合作用、蒸散作用

# ABSTRACT



Rainfall is one of the essential factors in affecting the inter-annual variability of vegetation productivity over tropical forests. However, it was reported that transpiration and productivity in tropical montane cloud forests with sufficient water are lower than in non-cloud tropical forests. By comparing the observational precipitation and vegetation indexes from satellite datasets, different water demand was found between Chi-Lan (CL) montane cloud forest and LienHuaChih (LHC) typical forest from January to April. More precipitation accumulation in November and December causes higher photosynthetic activities in LHC, while there is no significant change in CL.

We further conducted idealized sensitivity tests on precipitation in atmospheric forcing by using the land surface model to explore the critical factors affecting vegetation growth. The result shows that local microclimate dominates transpiration and photosynthesis, and a nonlinear response between the rainfall and gas exchange process in LHC corresponds to the soil water variation and vapor pressure deficit. No significant change in CL was found because of the stable and higher soil water content. Our study reveals that in non-cloud forests, vegetation photosynthetic activities in lower soil water periods could be affected by rainfall in the preceding months, while montane cloud forests are less susceptible because of sufficient water availability and less available solar energy. It could also indicate that in the future, with dry-get-drier climate conditions, montane cloud forests may be less influenced due to their relatively stable hydro-climatic conditions, especially from the water availability perspective.

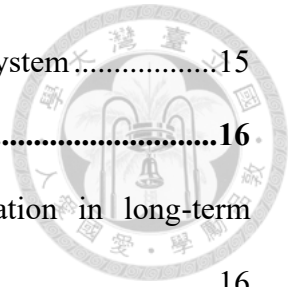
Keywords: cloud forest, precipitation, vegetation index, photosynthesis, transpiration

# CONTENTS



口試委員會審定書 .....	#
誌謝 .....	i
中文摘要 .....	ii
ABSTRACT .....	iii
CONTENTS .....	iv
LIST OF FIGURES .....	vi
LIST OF TABLES .....	x
<b>Chapter 1 Introduction.....</b>	<b>1</b>
<b>Chapter 2 Data and Methodology .....</b>	<b>4</b>
2.1 Site Description .....	4
2.2 Meteorological data .....	5
2.2.1 Observational Data.....	5
2.2.2 Taiwan ReAnalysis Downscaling data .....	5
2.3 Vegetation Indexes.....	6
2.3.1 Enhanced Vegetation Index (EVI).....	6
2.3.2 Leaf Area Index (LAI) .....	6
2.4 Potential Evapotranspiration Estimation .....	7
2.5 Model simulations .....	8
<b>Chapter 3 Results .....</b>	<b>11</b>
3.1 Vegetation might be sensitive to climate variables from January to April ...	11
3.2 Different water demand between two sites from January to April .....	12
3.3 Precipitation Sensitivity Test .....	13
3.3.1 Soil moisture variation and stomatal conductance.....	13

3.3.2	Microclimate is the main controlling factor to ecosystem.....	15
<b>Chapter 4</b>	<b>Discussion.....</b>	<b>16</b>
4.1	The relationship of vegetation indexes and precipitation in long-term perspective .....	16
4.2	Budyko curve.....	16
4.3	Scarcities in idealized sensitivity tests.....	17
4.4	Water and Carbon changes under the intensified precipitation .....	19
<b>Chapter 5</b>	<b>Conclusion .....</b>	<b>21</b>
FIGURES	.....	23
TABLES	.....	45
REFERENCE	.....	47



# LIST OF FIGURES

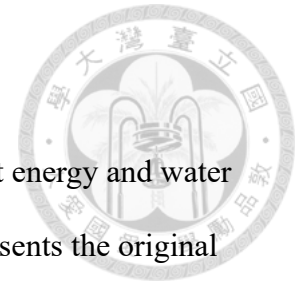


Figure 1.1 A schematic of Budyko diagram. The solid lines represent energy and water limits to the evaporative index, and the dashed line represents the original theoretical Budyko curve (after Budyko, 1974). (The figure is taken from Creed et al., 2014).....23

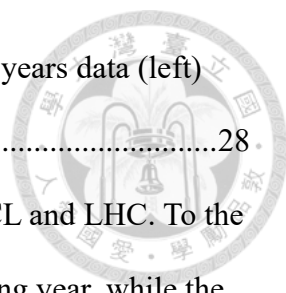
Figure 2.1 The location of the CL flux tower (red dot) and LHC flux tower (blue dot). The boxes around the flux tower indicates the area of two sides in our research, approximately 5km by 5km in size. ....24

Figure 2.2 Landtype comparison between CL and LHC. (The figure is taken from 古 (2020) and the middle Taiwan map is taken from Schulz et al. (2017)).....25

Figure 2.3 Precipitation seasonality in CL (2008-2011) and LHC (2008-2013). Solid lines present rainfall data from flux towers; dash lines are from TReAD data.....26

Figure 3.1 Seasonality of three plant hydrology related variables in CL and LHC. (a)(b) blue lines for precipitation; red lines for potential evapotranspiration (c)(d) four layers of soil moisture: dark to light gray color presents soil depth from surface to underground. ....27

Figure 3.2 The comparison of seasonality vegetation indexes during different year period in CL (orange lines) and LHC (blue lines): (a) EVI data, the averaged years matches the year of valid meteorological data from the flux tower (b) long-term EVI data from 2000-2020 (c) LAI data, the averaged years matches the year of valid meteorological data from the flux tower (d) long-term LAI data from 2000-2020 The shading colors represent the variation of



EVI/ LAI between first quartile and third quartile from 9 years data (left) and 20 years data (right). .....28

Figure 3.3 Month to month correlation between rainfall and EVI in CL and LHC. To the left of the dashed line present the precipitation in preceding year, while the right present current year to EVI. The blank space is VIs-leading condition, which are not to be considered. ....29

Figure 3.4 Month to month correlation between rainfall and LAI in CL and LHC. To the left of the dashed line present the precipitation in preceding year, while the right present current year to LAI. The blank space is vegetation-leading condition, which are not to be considered. ....30

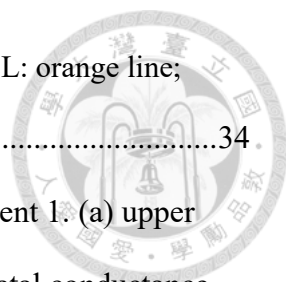
Figure 3.5 Scatter plot of average rainfall data in November and December and dry season vegetation indexes anomaly in CL (orange) and LHC (blue). The lines show linear regression results in each site. Both rainfall data are from in-situ flux tower. ....31

Figure 3.6 Scatter plot of average rainfall data in November and December and dry season vegetation indexes anomaly in CL (orange) and LHC (blue). The lines show linear regression results in each site. The rainfall data in LHC are from agricultural station, and rainfall data in CL are from in-situ flux tower. ....32

Figure 3.7 Comparison of LHC monthly rainfall from 2008 to 2016 between flux tower and agricultural station (AGR). The solid line presents linear regression between two datasets, and the p-value < 0.01. ....33

Figure 3.8 Results of dry season transpiration and photosynthesis from experiment 1. X-axis shows the multiple of Prec\_ND, and Y-axis are the change rate for





transpiration and photosynthesis compared to their CTR. (CL: orange line; LHC: blue line).....34

Figure 3.9 Results of four variables in dry season from from experiment 1: (a) upper 10cm soil water (b) vapor pressure deficit (c) sunlit stomatal conductance (d) shaded stomatal conductance (CL: orange line; LHC: blue line) Y-axis are the change rate for each variable compared to the CTR.....35

Figure 3.10 Results of four variables in dry season from experiment 1. (a) saturated vapor pressure (b) air vapor pressure (c) transpiration beta factor (d) CO<sub>2</sub> partial pressure (CL: orange line; LHC: blue line) Y-axes are the change rate for each variable compared to the CTR.....36

Figure 3.11 Results of dry season transpiration and photosynthesis from experiment 1 and 2. X-axis shows the multiple of Prec\_ND, and Y-axis are the change rate for transpiration and photosynthesis compared to their CTR. (CL: orange line; LHC: blue line; CLatm\_LHCsurf: red line; LHCatm\_CLsurf: dodgerblue line).....37

Figure 3.12 Results of dry season transpiration and photosynthesis from experiment 1 to 3. X-axis shows the multiple of Prec\_ND, and Y-axis are the change rate for transpiration and photosynthesis compared to their CTR. (CL: orange line; LHC: blue line; CLatm\_LHCsurf: red line; LHCatm\_CLsurf: dodgerblue line; CLclm\_LHCsurf: brown line; LHCclm\_CLsurf: lightblue line) .....38

Figure 3.13 Vapor pressure deficit seasonality calculated by observational flux tower data. Orange line for CL and blue line for LHC. Left picture are the was calculated by total time steps, while right picture only include daytime from 8a.m. to 5p.m. The shading colors represent the variation of VPD between first quartile and third quartile from 4 years in CL and 5 years in LHC. ....39

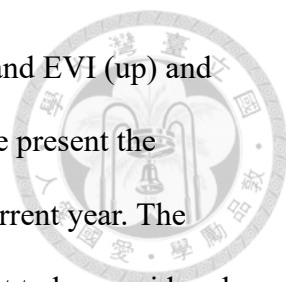


Figure 4.1 Month to month correlation between TReAD rainfall (P) and EVI (up) and LAI (down) in CL and LHC. To the left of the dashed line present the precipitation in preceding year, while the right present current year. The blank space is vegetation-leading condition, which are not to be considered.

.....40

Figure 4.2 Month to month correlation between TReAD surface temperature (T) and EVI (up) and LAI (down) in CL and LHC. The blank space is vegetation-leading condition, which are not to be considered. ....41

Figure 4.3 Month to month correlation between TReAD net radiation (Rn) and EVI (up) and LAI (down) in CL and LHC. The blank space is vegetation-leading condition, which are not to be considered. ....42

Figure 4.4 Monthly normalized potential evapotranspiration (PET) and actual evapotranspiration (AET) by precipitation in CL and LHC. Red circles present the calculation from January to April. Dash gray line represent energy and water limited. ....43

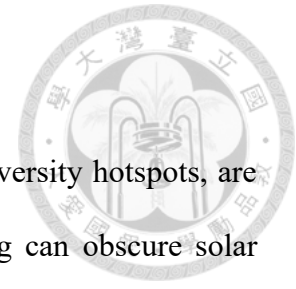
Figure 5.1 Schematic of low soil water period plant-water relation in tropical non-cloud forests, all the parameters derived from stomatal conductance formula in Community Land Model.....44

# LIST OF TABLES



Table 2.1 Experiment Design in CLM model simulation.....	45
Table 2.2 Daily average of multiple of November and December precipitation (Prec_ND) in CL and LHC .....	46

# Chapter 1 Introduction



Montane cloud forests, whose distribution overlaps with biodiversity hotspots, are characterized by a high frequency of fog. The high density of fog can obscure solar radiation and reduce the vapor pressure deficit (VPD) that develops, forming a distinctive hydro-climatological cycle and supporting the vulnerable ecosystem. Recently, montane cloud forests behave one of the most endangered forest types in the world under climate change. (Bruijnzeel et al., 2001; Mildenerger et al., 2009).

Gotsch et al. (2016) compared the water and carbon relations of lowland tropical forests and montane cloud forests, in which leaf light-saturated photosynthesis, transpiration, and vegetation productivity were mainly discussed from an ecosystem perspective. The plant water and carbon exchange in forests are inseparable since the transpiration process could open the stomata and thus allows carbon dioxide to diffuse into the air, completing a primary function of photosynthesis. The study shows that both transpiration and productivity in montane cloud forests are lower than in tropical forests (Gotsch et al., 2016). In montane cloud forests, reduced transpiration results in higher leaf wetness and soil water, implying that lower water demand and the shortage of photosynthetic active radiation may affect the greatest difference between cloud forests and non-cloud forests.

The insufficient radiation combined with abundant water could make montane cloud forests energy-limited, with the equilibrium between these two variables described by the concept of the Budyko curve (Fig. 1, Budyko, 1974). If the ratio of potential evapotranspiration (PET) to precipitation (P) is larger than the ratio of actual evapotranspiration (AET) to precipitation (P), the area is considered an energy-limited region. However, it has not been verified that montane cloud forests belong to energy-

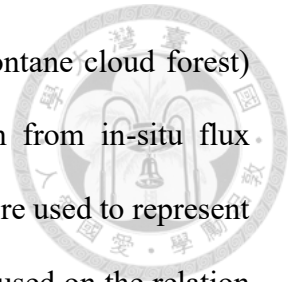
limited areas.

Precipitation has always played an important role in determining the water or energy-limited environment. Previous studies have shown that annual rainfall over a threshold of 1800 to 2000mm/yr can keep the photosynthetic activity in the dry season in tropical evergreen forests, meaning that vegetation in these areas can still grow (Guan et al., 2015, 2018). The phenomenon also indicates that water from the wet season can store in soil and support plant growth in the dry season. On the other hand, places with annual rainfall lower than the threshold do not have enough water availability from the soil in the dry season. Results from Chang et al. (2017) also show similarities. By doing correlation on Normalized Difference Infrared Index (NDII6, a satellite data which represents leaf water content) and the standardized precipitation index with a three-month time scale (SPI3, a drought index) in spatial scale, Chang et al. (2017) found a difference between southwestern (dry region) and northeastern Taiwan (wet region) in January and April. In northeastern Taiwan, where annual rainfall is larger than 2500mm/yr, the dry condition will not affect leaf surface wetness.

Chi-Lan (CL) montane cloud forest, located in northeastern Taiwan, receives approximately 4000mm/yr of rainfall and is frequently covered by fog and low-altitude clouds. Transpiration was suppressed by the frequent fog occurrence and in line with the net radiation rise, further resulting in photosynthesis activities. (Gu et al., 2021) Therefore, CL is a suitable place for studying how forest productivity changes and its linkage with micro-climatology. As a perhumid place with low energy input, we could hypothesize that CL is more like a radiation-limited place compared to the water-limited in non-cloud tropical forests. Hydrological processes and the ecosystem would be less sensitive to water changes without precipitation.

In this study, we aim to investigate the importance of rainfall to vegetation

photosynthesis by comparing two Taiwan forests, Chi-Lan (CL, montane cloud forest) and LienHuaChih (LHC, non-cloud forest). Monthly precipitation from in-situ flux towers and two kinds of satellite observational vegetation indexes were used to represent quantified photosynthetic capacity and vegetation greenness. We focused on the relation from January to April, a relatively drier periods for soil water in both sites. We hypothesized that montane cloud forests were not as required for water demand as tropical forests. Offline land model simulations in transpiration and net photosynthesis were also discussed to present the specific water and carbon flux.



## Chapter 2 Data and Methodology



To investigate the uniqueness of montane cloud forests, we compared two flux tower sites in Taiwan montane region: Chi-Lan montane cloud forest with frequent fog occurrence and LienHuaChih as a reference for a non-cloud forest. Two vegetation indexes are derived from satellite datasets for examining photosynthesis. Besides, to figure out the mechanism from rainfall to vegetation, offline land model experiments were designed.

### 2.1 Site Description

Chi-Lan montane cloud forest is located in northeastern Taiwan, being frequently immersed in afternoon fog happened at around 3 pm. Coniferous species are filled in this evergreen site, mostly dominated by Taiwan yellow cypress (*Chamaecyparis obtuse var. formosana*). CL flux tower (24°35'N, 121°25'E) was built on 14° mountain slope toward the southeast side (Fig. 2.1) at 1650m above mean sea level height, providing local meteorological and flux data, which was calculated by the eddy covariance method. Observational data from 2008 to 2011 and 2015 to 2019 shows the mean temperature is around 15°C, and the annual precipitation is more than 3300mm/yr. The precipitation in CL is usually associated with the lifting orographic cloud, which results from the warm air brought by valley wind. Typhoon and Mei-Yu season could lead to heavy rain in summer, while the cold front and northeast monsoon bring humid vapor to CL. (Chang et al., 2002; Klemm et al., 2006; Chu et al., 2014)

LienHuaChih presents a case of a non-cloud forest (mixed evergreen broadleaves) in central Taiwan, with 21°C in mean annual temperature and 2292mm/yr in precipitation from 2008 to 2016. LHC flux tower (23°55'52"N, 120°53'59"E) was built at 780m above mean sea level in sub-watershed No.5 at LHC Research Center (Chen and Li, 2012)

Precipitation seasonality in LHC is different from that of CL. The primary rainfall season in CL is from May to October, which gets a peak in October. LHC has significant seasonal variation, with the dry season from October to April and the wet season from May to September (Fig. 2.3).



## **2.2 Meteorological data**

### **2.2.1 Observational Data**

We accumulated half-hourly precipitation data to monthly one in CL flux tower and LHC flux tower. The period of CL dataset is 2008 to 2011 and 2015 to 2019, while the one in LHC is 2008 to 2016. The blank period in CL is because of the tower collapse in 2012, damaged during the typhoon season.

Besides precipitation, the other meteorological data were taken in fewer years in each site (CL: 2008 to 2011; LHC: 2009 to 2013) because of the maximum available data. Such as radiation, temperature, humidity, wind speed, and air pressure were used to calculate PET (Chapter 2.4, Fig. 3.2) and applied in land model simulation (Chapter 2.5).

### **2.2.2 Taiwan ReAnalysis Downscaling data**

Taiwan ReAnalysis Downscaling data (TReAD) is provided by the Taiwan Climate Change Projection Information and Adaptation Knowledge Platform (TCCIP), which is coordinated by the National Science and Technology Center for Disaster Reduction (NCDR). TReAD was dynamically downscaled from European Centre for Medium-Range Weather Forecasts (ECMWF) ERA5 reanalysis data by the WRF model. It provided a 2km resolution for each grid in hourly timescales from 1980 to 2020 in Taiwan. We used the TReAD as long-term data to make up for the shortage in flux tower observation.



## 2.3 Vegetation Indexes

We complemented two vegetation indexes products each other from 2001 to 2020: Enhanced Vegetation Index (EVI) from Terra Moderate Resolution Imaging Spectroradiometer (MODIS) and Leaf Area Index (LAI) from Copernicus Global Land Service (GLCS). Both products provide monthly and 1km resolution.

Vegetation indexes in our study present the photosynthetic ability, which are highly related to canopy transpiration, dominating evapotranspiration in tropical forests. We took the position of the flux tower as the center, selected an area of 5km by 5km outward, and then weighted averaged the indexes to represent the vegetation greenness state of the study sites.

### 2.3.1 Enhanced Vegetation Index (EVI)

We used MODIS-derived EVI data as a proxy of canopy photosynthetic capacities, according to Guan et al. (2015). EVI is an optimized vegetation index, which has been found to perform well with vegetation phenology. (Huete et al., 2002) Monthly 1km spatial resolution of EVI datasets (MOD13A3) was utilized in our research from 2000 to 2020, and it has minimized canopy background variation, being more sensitive to vegetation measure. We extracted image-transform to numerical EVI datasets online at the Application for Extracting and Exploring Analysis Ready Samples website (AppEEARS, <https://lpdaacsvc.cr.usgs.gov/appears/>), which provides geospatial data with customized spatial, temporal, and band/layer parameters.

### 2.3.2 Leaf Area Index (LAI)

LAI is widely used to describe vegetation development in ecosystems and can determine the ability of photosynthetic degree and evapotranspiration. We planned to compare the performance of LAI with EVI, then observe the mutually impacted

precipitation timestep to vegetation in our study period. For comparison, we used LAI data from the European Space Agency (ESA) instead of the MODIS-derived one. ESA LAI was obtained from The Copernicus Global Land Service website (CGLS, <https://land.copernicus.eu/global/products/lai>), which provides a global land-monitoring dataset. Two kinds of products, SPOT/VGT (1999-2013) and PROBA-V (2014-2020), were combined as long-term observations for each grid. 10-days LAI index has been validated with other global products and removed the contamination from clouds and snow. ESA LAI has a high correlation with in-situ observational LAI and performs better vegetation phenology than MODIS LAI in tropical evergreen areas (Brown et al., 2020; Gessner et al., 2013).

## 2.4 Potential Evapotranspiration Estimation

Potential evapotranspiration (PET) can be derived from atmospheric conditions without considering the available water supply. Penman-Monteith Equation and Priestley-Taylor Equation are primarily used in PET estimation (Monteith 1965, 1979; Allen et al., 1998; Priestley & Taylor, 1972). Priestley-Taylor Equation was more simplified than Penman-Monteith Equation; the vapor pressure deficit and convection term seemed as constant, easily with bias in drier conditions (McAneney & Itier, 1996). As a result, Penman-Monteith Equation is more suitable for comparing cloud and non-cloud forests. We need meteorological data such as net radiation, temperature, humidity, wind speed, and air pressure. Because of the maximum availability of observational data, calculation in CL was from 2008-2011 and LHC from 2009-2013. (Eq. 1)

$$PET = \frac{\Delta(Rn-G) + \rho_a c_p \frac{e_s - e_a}{r_a}}{\Delta + \gamma(1 + \frac{r_c}{r_a})} \quad (\text{Eq. 1})$$

$\Delta$  : slope of the vapor pressure curve



$R_n$  : net radiation

$G$  : ground evaporation

$e_s - e_a$  : vapor pressure deficit

$\rho_a$  : mean air density at constant pressure

$c_p$  : specific heat of the air

$\gamma$  : psychrometric constant

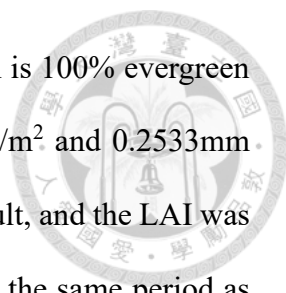
$r_a$  : aerodynamic resistance

$r_c$  : surface resistance

Ground evaporation and surface resistance could be neglected in CL due to the saturated soil water surface. In LHC, ground evaporation derived by Community Land Model (Chapter 2.5) is about 12% of net radiation in average ( $G_{LHC} \approx 0.12R_n$ ). We took 24.8 (mm/s) for surface conductance ( $1/r_c$ ) in LHC as the value was suggested for maximum surface conductance for tropical forests. (Tan et al., 2019)

## 2.5 Model simulations

We ran Community Land Model (CLM, Version 5) to simulate transpiration (decomposed from latent heat flux) and photosynthesis, which two variables have been compared in the previous study (Gostch et al., 2016) and cannot be easily measured in observational data. We mapped a 2X2 degree area as the proxy for a single point in each site, putting the same value in each grid, with CL (2008-2011) and LHC (2009-2013) flux tower observational data. Half-hourly data of precipitation, downward shortwave radiation, temperature, surface pressure, specific humidity, wind speed, and downward longwave radiation were used as the atmospheric forcing for the land model. Missing values were filled by their climatology each time step.



We followed the CL landtype setting by Gu et al. (2021), which is 100% evergreen needleleaf temperate tree with a yearly mean LAI of around  $4.3\text{m}^2/\text{m}^2$  and  $0.2533\text{mm}$  maximum allowed dew. The landtype in LHC was set by model default, and the LAI was adjusted to  $3.95\text{m}^2/\text{m}^2$  on a yearly average. The forcing ran once in the same period as the forcing year, and we removed the first-year simulation because of the spin-up mechanism. Transpiration and total photosynthesis were mainly discussed, which present the gas exchange process from vegetation to the atmosphere in hydrology and ecology, respectively.

Three idealized experiments were conducted in two sites. (Table 1) We firstly multiplied November and December precipitation values (Prec\_ND) by 10% to 150% without changing other climate variables (Exp 1). To investigate the variation, we subtracted with the control run one (CTR, precipitation value times 100%) and normalized it in each case. Second, to ensure how the landtype difference influence local photosynthesis, Experiment 2 (Exp 2) was conducted by exchanging CL and LHC landtype. That is, CL would involve in a significant seasonal variation while LHC turned into a constantly humid area.

In the third experiment (Exp 3), we exchanged all other atmospheric forcing but only kept local Prec\_ND for multiplying in the sensitivity test. For example, in LHCclm\_CLsurf, abundant water was input in November and December, while the plants obtained more light and were in a warmer atmosphere. In the other case, rainfall became smaller in November and December, with a cooler and humid environment all year. This experiment could tell us how the sudden more/less rainfall would influence local soil variability and, thus ecosystem when it was already in dry/humid conditions. We chose the same period in the atmospheric forcing from 2009 to 2011 in each site to avoid the different synoptic weather conditions by interannual variability. Both cases were

simulated repeatedly for six years, and the data in the last three years were analyzed in Exp3.



## Chapter 3 Results

### 3.1 Vegetation might be sensitive to climate variables from January to April



To determine the dry season in both sites, we discussed the three conditions from hydrological and ecological perspectives. The comparison of local monthly PET and precipitation was first considered (Fig. 3.1(a); Fig3.1(b)). PET was derived from meteorological variables from in-situ flux towers and defined as maximum evaporation under a sufficient water source. LHC has a significantly seasonal variation, with a long dry period from September to April. On the contrary, with a higher value in precipitation than PET, there is no obvious dry season found in CL in this aspect, except for the very close value in April.

We then secondly looked into soil moisture, which means the water content of the soil (Fig. 3.1(c); Fig 3.1(d)). Soil moisture is a key factor in controlling the water and heat fluxes through evapotranspiration, and it also provides the water for photosynthesis. Due to the humid environment and shallow soil depth, soil moisture is always stable in CL. In contrast, a large seasonal variation was shown in LHC, meaning the place was easily affected by water input. It can be noticed that both CL and LHC have lower soil moisture from January to April, which also overlaps with the lower difference between PET and rainfall in CL and a part of the dry period in LHC.

The inter-annual standard deviations in EVI and LAI were investigated from the ecological perspective. EVI and LAI have apparent seasonal variation, and they peak in July while being lowest in January (Fig. 3.2). The primary growing months start in April, supposedly the driest month in soil moisture. A larger variation was found from January to April, indicating that vegetation in each site is more susceptible to environmental

factors during this dry period.

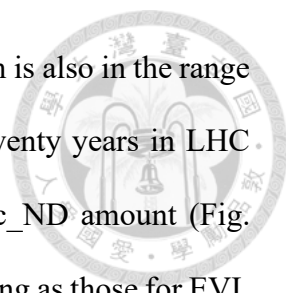
### **3.2 Different water demand between two sites from January to April**



The dominant precipitation period to EVI and LAI in the water period was determined by Pearson correlation with monthly datasets (Fig. 3.3). Under the influence of the precipitation in the preceding year, especially from October to December, there is a strong correlation with EVI anomaly, indicating a delayed response between precipitation and photosynthesis. In CL, the precipitation at the end of the previous year has a negative effect on EVI of the following months (Jan-Apr), while it is a positive in LHC. This relationship can also be seen in LAI results in the preceding November to December (Prec\_ND) (Fig. 3.4). A difference is that the correlation of LAI is not as strong as that of EVI, the positive effect of LHC is smaller, and the negative effect in EVI turns to no correlation in CL ( $R < 0.4$ ).

Focusing on the interannual variation of each month, we subtracted vegetation indexes with their climatology, and investigated anomaly value as the change degree (Fig. 3.5). Since LAI is calculated by the area of foliar as an indicator, it may not change significantly in tropical evergreen forests. In terms of vegetation greenness, the two sites show different slope signs from the regression, implicating their characteristics on water demand. From Jan. to Apr., LHC PET is greater than the precipitation value, meaning that local plants suffer from water shortage, and photosynthesis is highly affected by water. During the same period in CL, though it is drier than the state of the whole year, due to sufficient water, photosynthesis may saturate, resulting in a negative or no significant response with precipitation.

In addition, LHC Agricultural Station has long-term precipitation data, and its



location is about 2.5 kilometers away from the LHC flux tower, which is also in the range of 25km<sup>2</sup> area that we applied for vegetation indexes. Results of twenty years in LHC show the vegetation indexes change significantly, followed by Prec\_ND amount (Fig. 3.6). Although the flux tower regression results for LAI are not as strong as those for EVI, the long-term regression results suggest that Prec\_ND may impact LAI next year. In summary, when only considering the effect of water to vegetation in the drier period, photosynthesis in CL is less sensitive to water input, but the one in LHC is.

### **3.3 Precipitation Sensitivity Test**

#### **3.3.1 Soil moisture variation and stomatal conductance**

In the model simulation, we mainly discussed transpiration and total photosynthesis from January to April, presenting water and carbon gas exchange, respectively, from hydrological and ecological perspectives. Both two variables show similar changes with the observational results. A significant rising trend followed by increasing Prec\_ND is shown in the LHC, while it tends to zero in CL (Fig. 3.8).

The water supply for plants' internal water transport depends on soil moisture. LHC soil moisture rises linearly before the CTR, meaning the added rainfall can wet the dry soil in the following month (Fig. 3.9(a)). In contrast, CL has a little increase in soil water from 0.1Prec\_ND to 0.3Prec\_ND, but the rest of the tendency is stable, meaning the soil water has already saturated.

The Stomatal state has a direct response to both transpiration and photosynthesis. Stomatal conductance ( $g_s$ ) can be a proxy of the stomatal opening degree, which influences the gas exchange above the canopy. In CLM5.0, stomatal conductance was derived by three variables by using Medlyn stomatal conductance model: net leaf photosynthesis rate ( $A_{net}$ ), vapor pressure deficit (VPD), and CO<sub>2</sub> concentration. (Eq. 2,



Medlyn et al. 2011) As CO<sub>2</sub> partial pressure here is constant, stomatal conductance was determined by VPD and A<sub>net</sub>. (Fig. 3.10(d))

$$g_s = g_0 + 1.6\left(1 + \frac{g_1}{\sqrt{D}}\right) \frac{A_{net}}{c_s/P_{atm}} \quad (\text{Eq. 2})$$

$g_0$  : minimum stomatal conductance ( $\mu\text{mol}/\text{m}^2\text{s}$ )

$g_1$  : plant functional type dependent parameter (de Kauwe et al. 2015)

$A_{net}$  : net leaf photosynthesis rate ( $\mu\text{mol CO}_2/\text{m}^2\text{s}$ )

$c_s$  : CO<sub>2</sub> partial pressure at the leaf surface (Pa)

$P_{atm}$  : atmospheric pressure (Pa)

$D$  : vapor pressure deficit at the leaf surface (kPa)

VPD is the subtraction of saturated vapor pressure ( $e_s$ ) and air vapor pressure ( $e_a$ ), the drier environment results in higher VPD, and thus the stomata close in order to retain the internal water. Our tests show that adding water lowers the  $e_s$  but makes  $e_a$  higher, which results in VPD reduction, turning LHC into a wetter place so that the transpiration could get faster (Fig. 3.10(a); Fig3.10(b)). However, the VPD value in CL is inherently low, representing a very humid environment, so the transpiration could not process efficiently (Fig. 3.13).

The transpiration beta factor (value from 0 to 1) is a function of A<sub>net</sub>, which can reflect on the plants' hydraulic stress. It represents the ability of water transport from soil water to transpiration; the higher the value is, the vegetation more unstressed to water. In LHC case, the transpiration beta factor is highly following the soil water change in the beginning but turns to constant later (Fig. 3.10(c)). The changes in beta factor complementarity with VPD may be one of the reasons for the nonlinear trend. Initially, VPD and transpiration beta factor changes fast, making stomata open easily. When it is wet in the later stage, it can be seen that both two parameters slow down though the soil



moisture still rises rapidly. If the transpiration beta factor remains constant, it means that the supply of water is fixed. VPD would then be a regulating factor in the whole process.

### 3.3.2 Microclimate is the main controlling factor to ecosystem

By comparing experiment 1 and 2, we confirmed that surface characteristics rarely affect forests ecosystem rather than atmospheric factors (Fig. 3.11). CLatm\_LHCsurf was nearly zero changes, while the variety in LHCatm\_CLsurf shows a similar pattern to LHC case in EXP1. Local microclimate plays a critical role in maintaining the forest ecosystem and may dominate the hydrological and ecological difference between CL montane cloud forest and LHC non-cloud forest. The phenomenon has also verified the speculation in the previous study (Gotsch et al., 2016).

Experiment 3 was conducted to present the importance of soil moisture variability (Fig. 3.12). Simulations forced by CL atmospheric forcing are stable in transpiration and photosynthesis no matter how less or more rainfall was input. In contrast, climatology in LHC has a significant dry and wet season, which involves a very dry state at the beginning (0.1Prec\_ND), resulting in a large variation in soil moisture under precipitation changes. A higher amount of rainfall input sharply increases the soil water and then gets saturated at 0.5Prec\_ND, which is about twice the amount of CTR Prec\_ND in LHC flux tower data. Transpiration and photosynthesis tend to be constant after 0.3Prec\_ND though soil water is still increasing. This infers that even in non-cloud forests, subsurface soil water supply to vegetation might be larger than water loss via transpiration and photosynthesis, so water and carbon gas change could get to an upper limit, thus transforming to energy limit condition.

## Chapter 4 Discussion



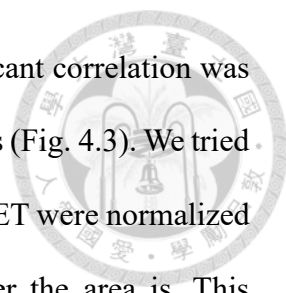
### 4.1 The relationship of vegetation indexes and precipitation in long-term perspective

Since the rainfall data in the flux tower only have nine years in each site without totally overlapped, a concern was raised about the data shortage. Would the relationship between Prec\_ND and vegetation growth in the dry-soil season also show in a longer period? To cope with the data with EVI and LAI (2001-2020), we used Taiwan ReAnalysis Downscaling data (TReAD) to verify our result. Precipitation data in TReAD can interpret seasonal variation well with completely flux tower data ( $R^2 = 0.93(\text{CL})$ ,  $0.96(\text{LHC})$ ) though there is some underestimation in October (Fig. 2.3).

Pearson correlation value in 20 years seems less robust than the observational ones (Fig. 4.1). It still can be seen that the two sites are requesting the different water demands between Prec\_ND and vegetation indexes during the lower soil water period, especially in EVI. Prec\_ND has a positive response to the vegetation indexes in LHC. CL has a little negative effect on November rainfall and EVI, but mostly no significant correlation between those two. Surface temperature and net radiation were also taken into consideration for the same phase correlation (Fig. 4.2; Fig. 4.3). Surface temperature has a significant positive response to EVI from January to March in CL, indicating that energy is more important to vegetation photosynthetic capacity than water. It could be noticed that the relationship between net radiation and vegetation indexes is very weak, mostly in all places.

### 4.2 Budyko curve

Gu et al. (2021) claimed that transpiration is in the same phase with net radiation



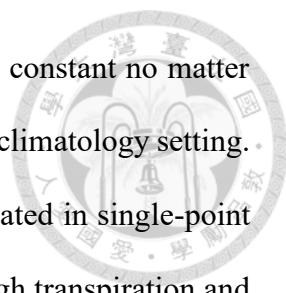
because photosynthesis process in diurnal scale; however, no significant correlation was shown between net radiation and vegetation indexes in TReAD results (Fig. 4.3). We tried to analyze observational data to the Budyko curve, where PET and AET were normalized by precipitation, respectively. The higher value of PET/P, the drier the area is. This method can distinguish whether evapotranspiration is affected by light in the case of sufficient water. When the ratio falls around the 1:1 line, the evapotranspiration is dominated by energy; On the contrary, when the PET/P exceeds 1, it becomes water-limited (Fig. 1.1).

The algorithm for calculating the Budyko curve is mostly year by year. Unfortunately, there are only 4 to 5 years of observational data for our calculation, so we averaged the data in monthly climatology, avoiding overmuch missing values. (Fig. 4.4). A large proportion of points fall around the energy-limited line in CL, while points in LHC are primarily out of the 1:1 line. The ratio of PET/P is always at a very high value because of the small daily precipitation value. Here, we removed the value PET/P larger than 5 and compared the percentage of energy-limited points to all valid points. Both two sides had removed half of the total data.

For all the valid months, 93% of points in CL are energy limited, while 58% are in LHC. When it comes to January to April, there are 80% energy-limited points and only 30% in LHC. We could roughly determine that CL is more energy-limited than LHC. Though we tried to use daily climatological data to distinguish whether CL is an energy or water-limited place, it is still uncertain because of the less data.

### **4.3 Scarcities in idealized sensitivity tests**

The idealized tests did not take into realistic weather conditions account, so there are many uncertainties that need to be discussed. First, in our model simulation, LAI and



productivity changes were not simulated effectively. LAI value kept constant no matter how we changed the atmospheric forcing. It was maintained with the climatology setting. Moreover, many parameters of biological processes cannot be simulated in single-point simulations, such as respiration and net primary productivity. Although transpiration and total photosynthesis can be seen in our results, they can only reflect the partial mechanisms in the biological process. Therefore, transpiration can better show the efficiency of current plant gas exchange than photosynthesis in our study.

Second, other atmospheric variables should be considered for reasonable weather conditions. For example, fog's effect can suppress the CO<sub>2</sub> uptake in cloud forests. (古, 2020) However, as previously discussed, biological parameters are mostly not simulated in our experiments. Besides fog and precipitation, specific humidity, air temperature, and radiation could be very different from 0.1 times precipitation to 1.5 times precipitation. The idealized experiments were conducted in all the same energy conditions. On the other hand, temperature could also affect vegetation growth, as we have discussed previously from the TReAD correlation result (Chapter 4.1). The impacts of multiple factors coupling to the gas change process would be the priority discussion in the future.

Third, Prec\_ND was decided by Pearson correlation results on rainfall and vegetation indexes in observational data. It is not sure if earlier months (e.g., October and more precede months) could affect the vegetation or not. For example, the correlation result in CL shows that October also has a negative effect on spring EVI (Fig. 4.2(a)). The lag responses between rainfall and vegetation in two kinds of forests could possibly be explained if we conduct more tests at different temporal scales.

## 4.4 Water and Carbon changes under the intensified precipitation



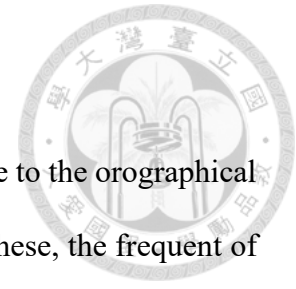
Recent studies have discussed how would climate changes influence cloud forests. The net photosynthesis rate increase because of easier CO<sub>2</sub> absorption through the rising CO<sub>2</sub> concentration, and the efficiency of photosynthesis becomes higher. (Ainsworth and Rogers, 2007) The rising temperature might decrease the relative humidity in cloud forests, reducing the formation of fog. (Foster, 2001; Still et al., 1999) Besides, lower humidity will increase vapor pressure deficit, which in turn increases stomatal conductance, making transpiration more efficient. (Stewart, 1988) From hydrological perspective, in some tropical cloud forests with significant seasonal variation in precipitation, fog interception can maintain water storage in soil, supporting vegetation growth even in the dry season. (Dawson & GoldSmith, 2018; Limm et al., 2012; Sepúlveda et al., 2018) Decreasing in fog occurrence may pose a threat to those regions.

In the cool season, October to April, the fog also has a remarkable proportion in CL hydrology (Chu et al., 2014), which overlaps with our study time period. However, our study has shown that, in CL, a high amount of precipitation provided abundant water to local vegetation. This includes that fog can reduce the energy input instead of being a water input factor, making CL always an energy limit place. The shortage of fog immersion under climate change probably does not impact the available water to CL cloud forests, or it can positively grow trees better due to higher accessed solar energy.

In the future climate projection in Taiwan, the dry season gets drier, especially in spring. The decreased water availability might pose a threat to non-cloud forests, making plants hardly conduct the photosynthesis process. Conversely, montane could forests might have an effective photosynthesis process meanwhile because of less water input.

The increasing number of non-rainy days could evaporate the redundant water, rising the vapor pressure deficit value in montane cloud forests. Furthermore, local plants might earn more solar radiation because of fog dissipation. The gas exchange between leaves and the atmosphere could be more effective. This makes montane cloud forests play an important role as a carbon sink in the ecosystem. Still, the multiple climate factors that impacted the photosynthetic process in this period should be discussed more.

## Chapter 5 Conclusion



CL montane cloud forest has a large amount of precipitation due to the orographical rainfall, northeastern monsoon systems, and winter fronts. Besides these, the frequent occurrence also provides horizontal interception and reduces solar radiation, making soil moisture almost saturated all year round. This humid environment allows vegetation to thrive even during non-rainy seasons without experiencing water shortages. In contrast, LHC non-cloud forest has distinct seasonal variation in soil water, so water availability during the non-rainy season could have a strong impact on the local ecosystem.

We found that the photosynthetic capacity was sensitive to the meteorological factor from January to April (low soil water periods) from the analysis of observational rainfall data and vegetation indexes. Water sources from precipitation in the preceding November and December can easily influence LHC non-cloud forest, with the lag response of precipitation variations to the soil. In contrast, CL montane cloud forest seemed less susceptible to water input.

The precipitation sensitivity tests confirmed that local microclimate characteristics dominate the vegetation greenness state compared to the changes in the land type and species. Instead, stomatal conductance and soil water content play important roles in controlling gas exchange. Stomatal conductance is affected by water transport from soil to vegetation and vapor pressure deficit, which restrain each other and regulate the stomata closure (Fig. 5.1).

Our study focused on the relationship between precipitation and vegetation. However, other climate variables, such as temperature and solar radiation, may also affect forest productivity. By considering these factors, we could better understand whether CL montane cloud forest is sensitive to energy factors in non-rainy seasons. Only then could



we know whether CL montane cloud forest is sensitive to energy factors in non-rainy seasons.

Also, the biogeochemical mechanism of photosynthesis still accounts for a crucial part that needs further investigation. It is unclear whether cloud forests will be able to function as vital carbon sinks under future climate change or if they will become vulnerable to multiple climate change factors. More idealized model simulations and observational-based data may be necessary to fully understand plant water relations in these ecosystems.

## FIGURES

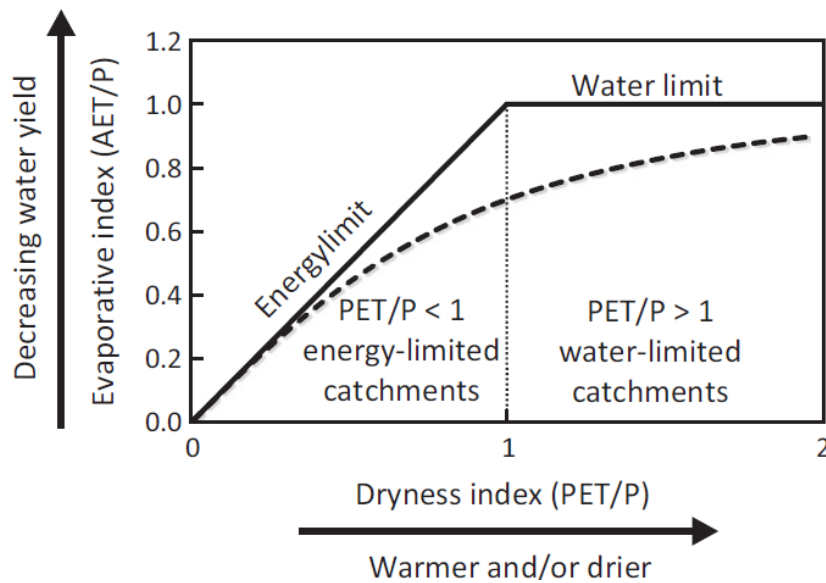


**Figure 1.1** A schematic of Budyko diagram. The solid lines represent energy and water limits to the evaporative index, and the dashed line represents the original theoretical Budyko curve (after Budyko, 1974). (The figure is taken from Creed et al., 2014)

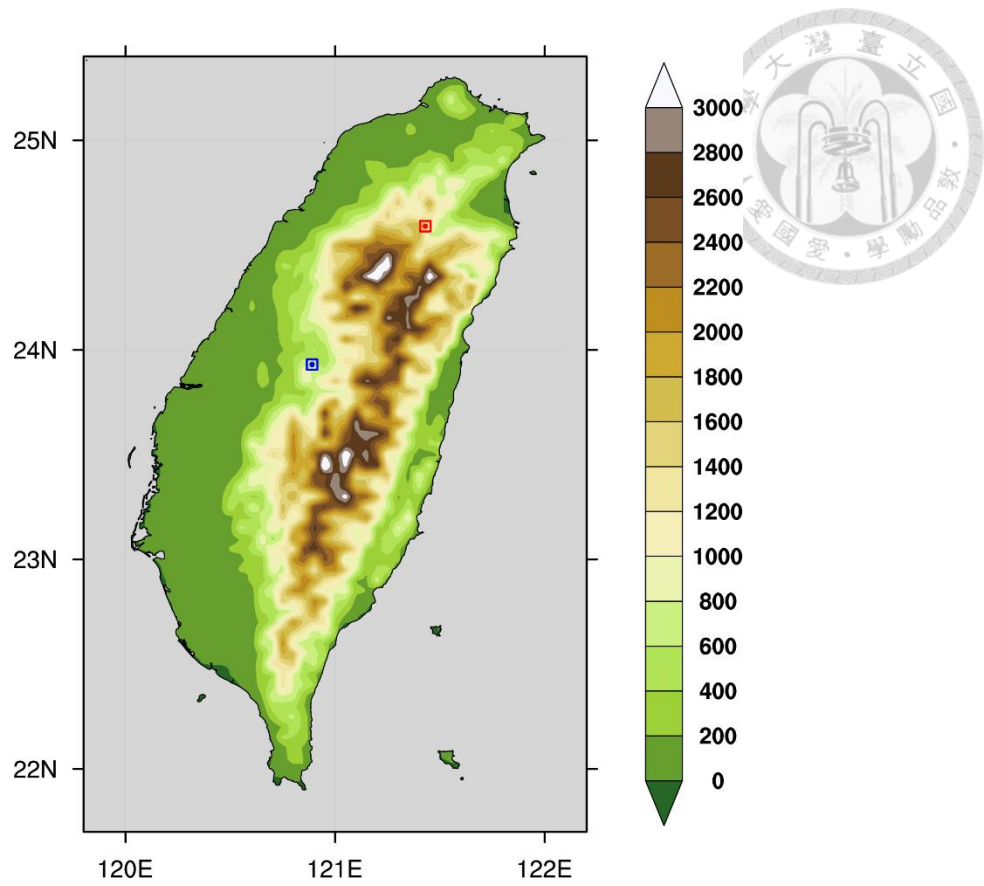


**Figure 2.1** The location of the CL flux tower (red dot) and LHC flux tower (blue dot).

The boxes around the flux tower indicates the area of two sides in our research, approximately 5km by 5km in size.

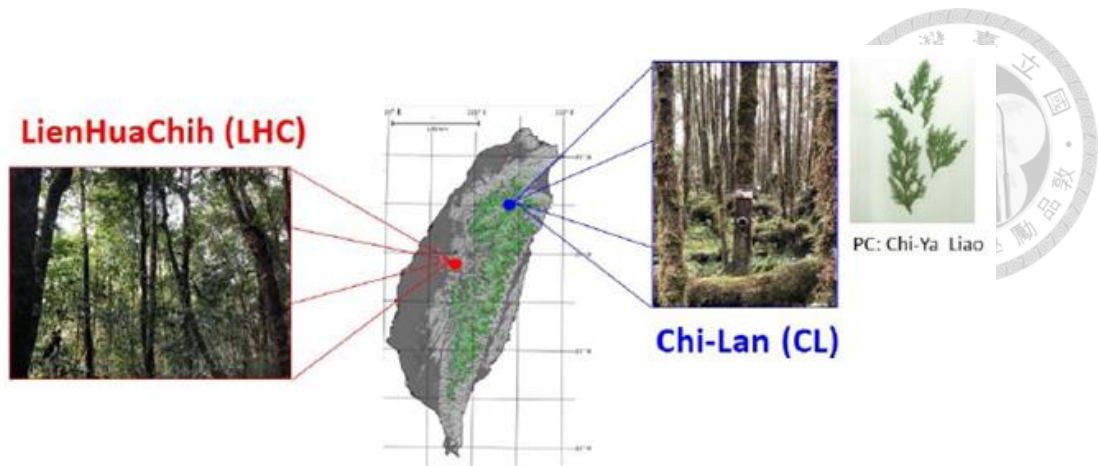


**Figure 2.2** Landtype comparison between CL and LHC. (The figure is taken from 古 (2020) and the middle Taiwan map is taken from Schulz et al. (2017))

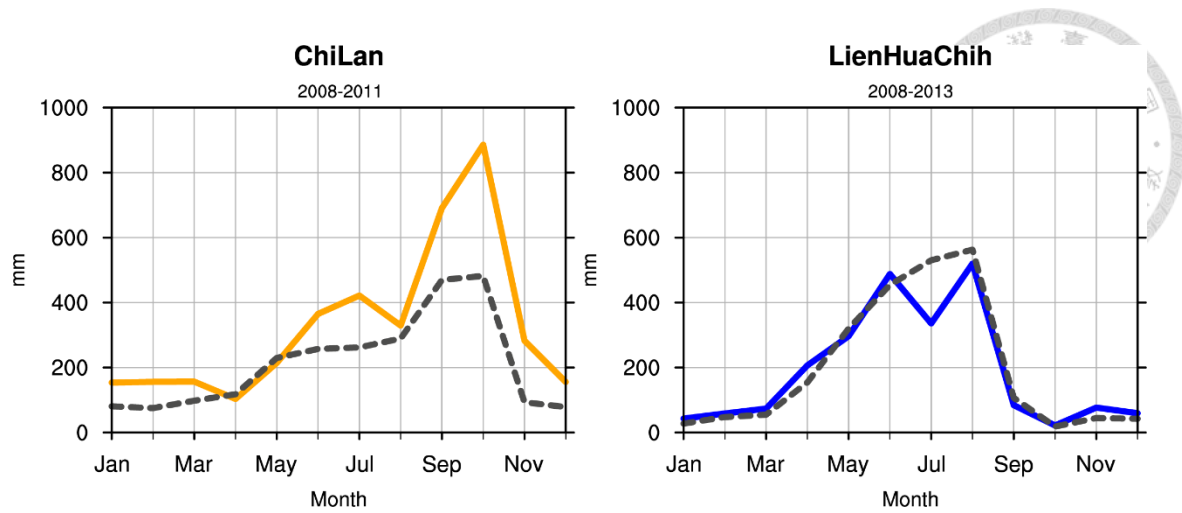


**Figure 2.3** Precipitation seasonality in CL (2008-2011) and LHC (2008-2013). Solid lines present rainfall data from flux towers; dash lines are from TReAD data.

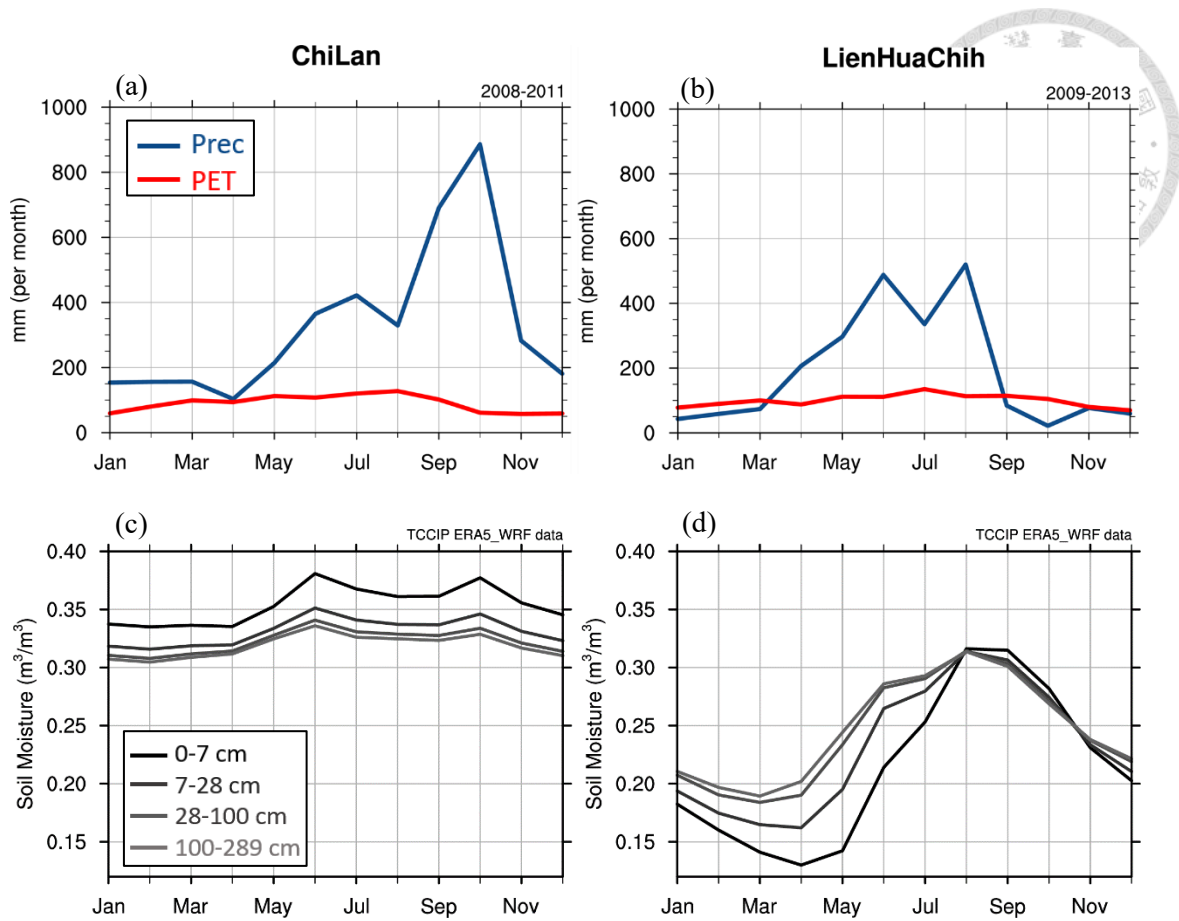


**Figure 3.1** Seasonality of three plant hydrology related variables in CL and LHC.

(a)(b) blue lines for precipitation; red lines for potential evapotranspiration (c)(d) four layers of soil moisture: dark to light gray color presents soil depth from surface to underground.

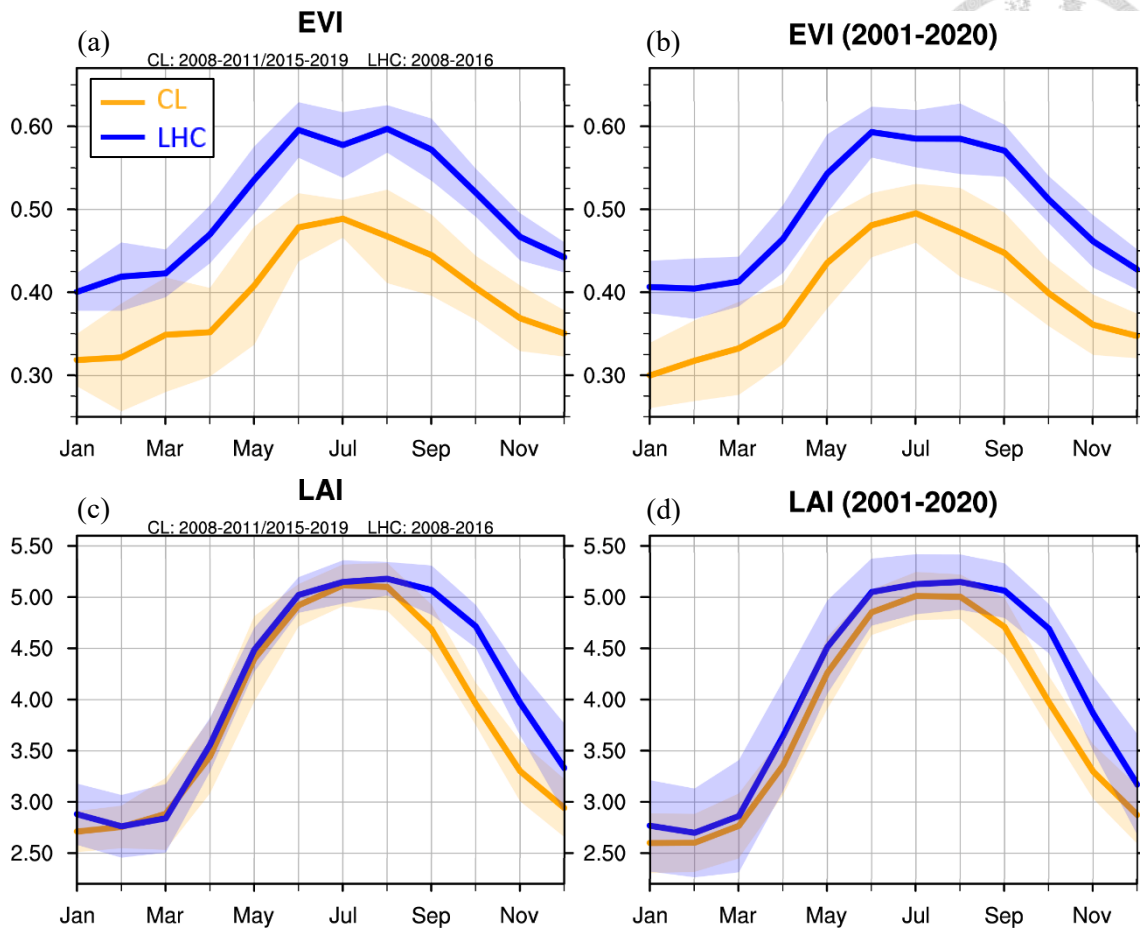


**Figure 3.2** The comparison of seasonality vegetation indexes during different year period in CL (orange lines) and LHC (blue lines): (a) EVI data, the averaged years matches the year of valid meteorological data from the flux tower (b) long-term EVI data from 2000-2020 (c) LAI data, the averaged years matches the year of valid meteorological data from the flux tower (d) long-term LAI data from 2000-2020 The shading colors represent the variation of EVI/ LAI between first quartile and third quartile from 9 years data (left) and 20 years data (right).

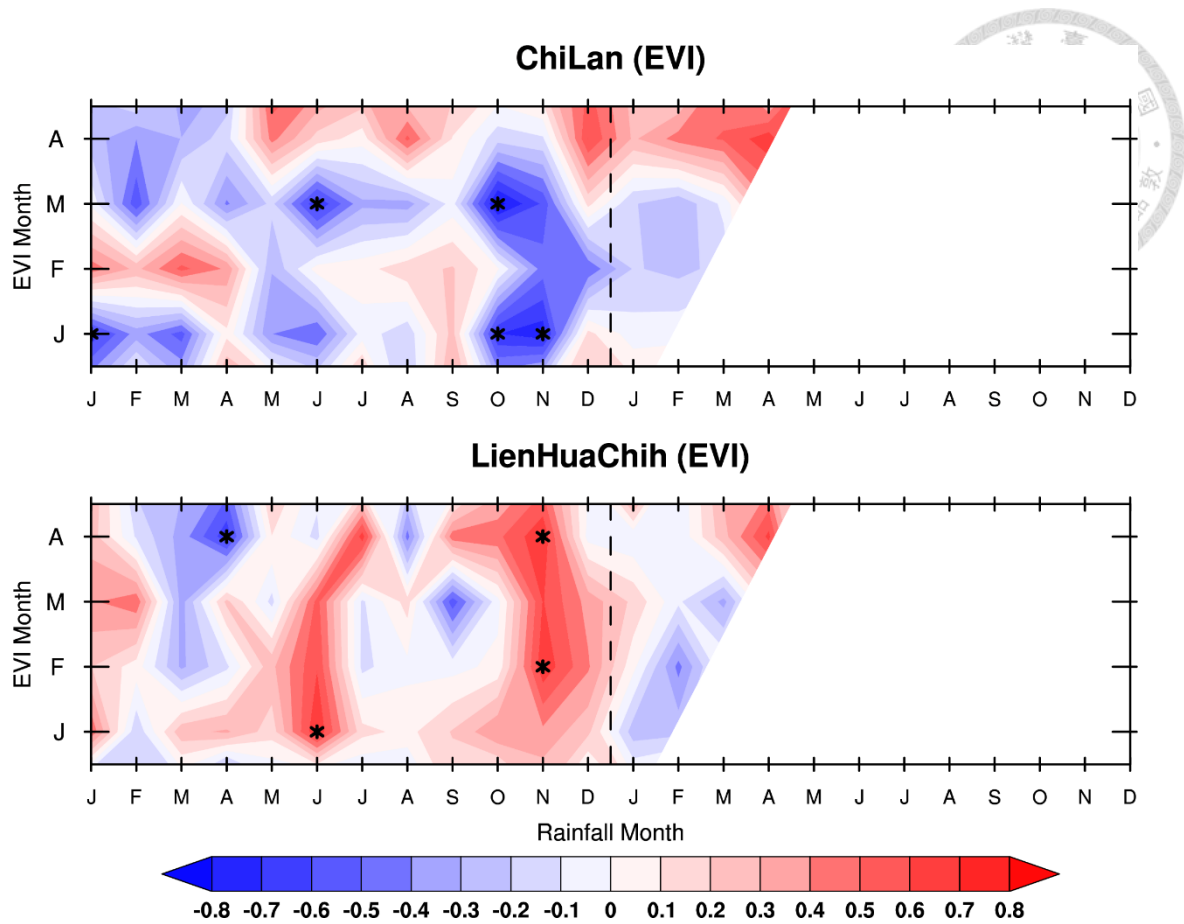


**Figure 3.3** Month to month correlation between rainfall and EVI in CL and LHC.

To the left of the dashed line present the precipitation in preceding year, while the right present current year to EVI. The blank space is VIs-leading condition, which are not to be considered.



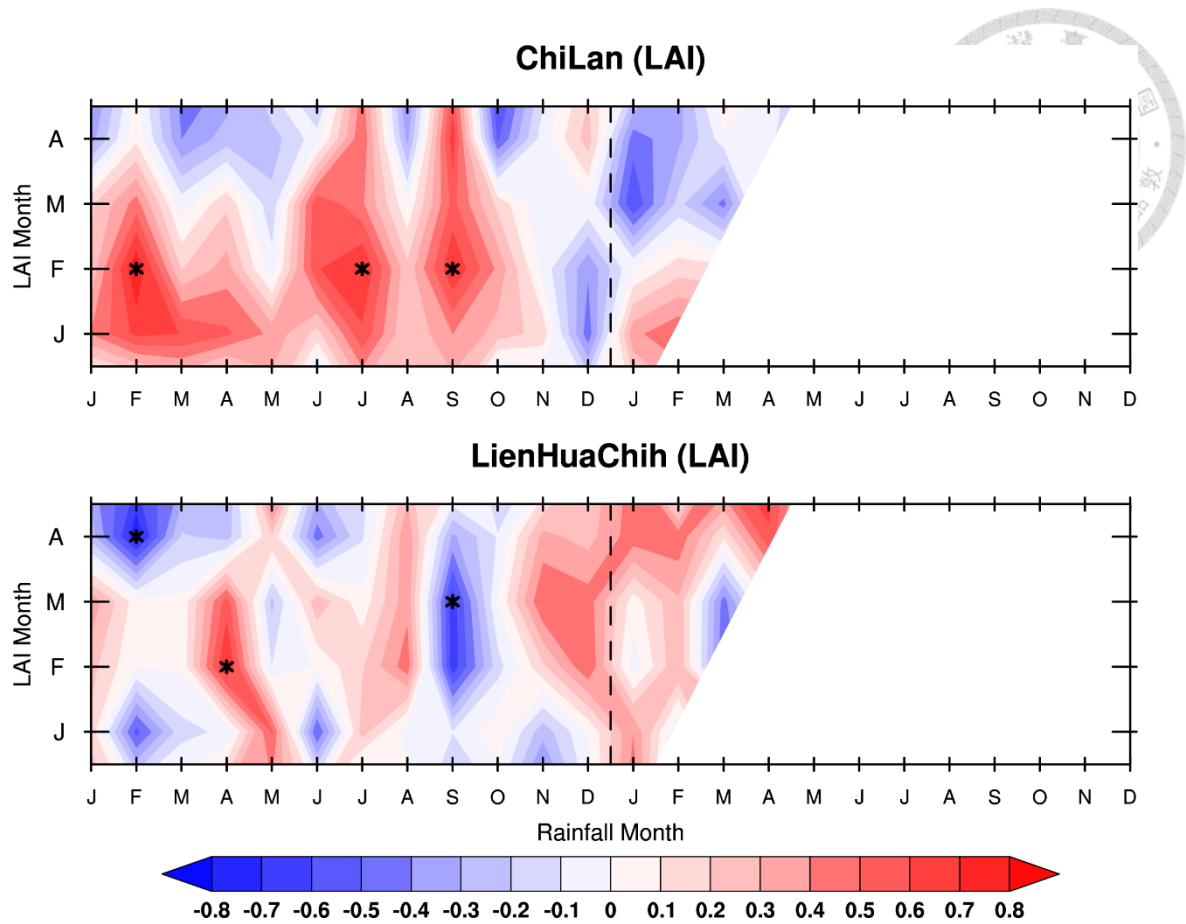


**Figure 3.4** Month to month correlation between rainfall and LAI in CL and LHC.

To the left of the dashed line present the precipitation in preceding year, while the right present current year to LAI. The blank space is vegetation-leading condition, which are not to be considered.

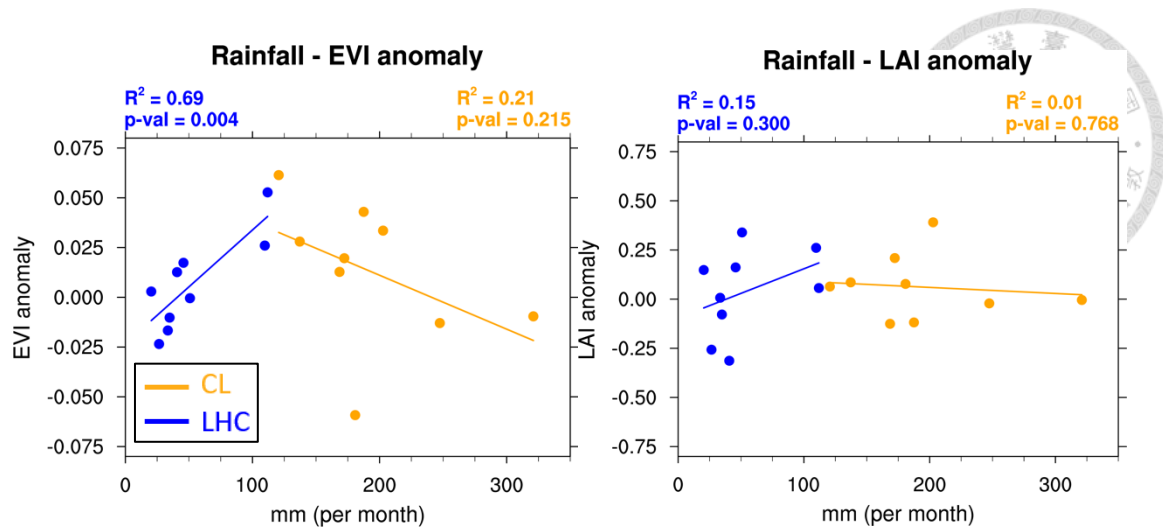


**Figure 3.5** Scatter plot of average rainfall data in November and December and dry season vegetation indexes anomaly in CL (orange) and LHC (blue). The lines show linear regression results in each site. Both rainfall data are from in-situ flux tower.

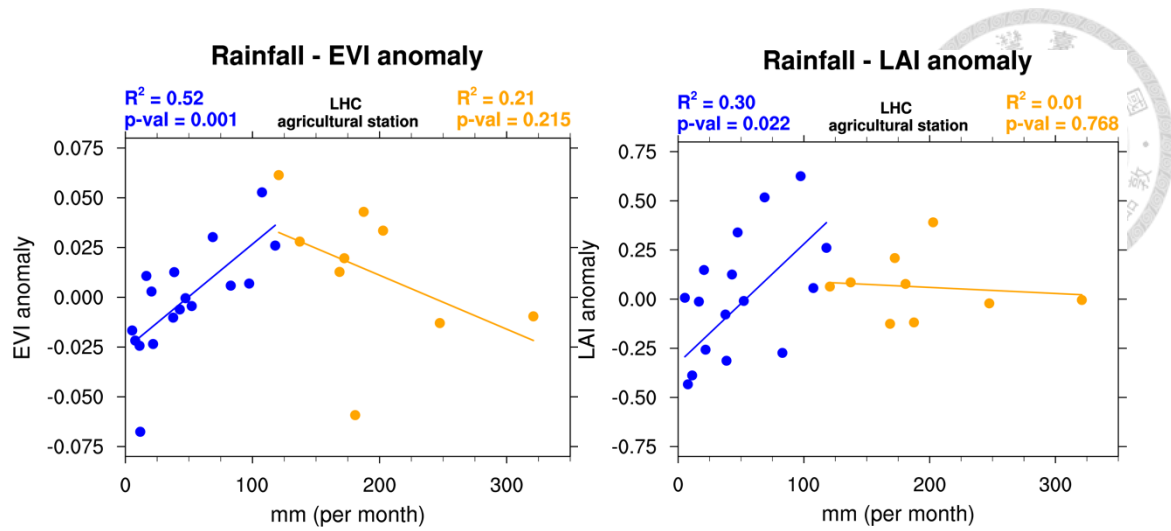


**Figure 3.6** Scatter plot of average rainfall data in November and December and dry season vegetation indexes anomaly in CL (orange) and LHC (blue). The lines show linear regression results in each site. The rainfall data in LHC are from agricultural station, and rainfall data in CL are from in-situ flux tower.

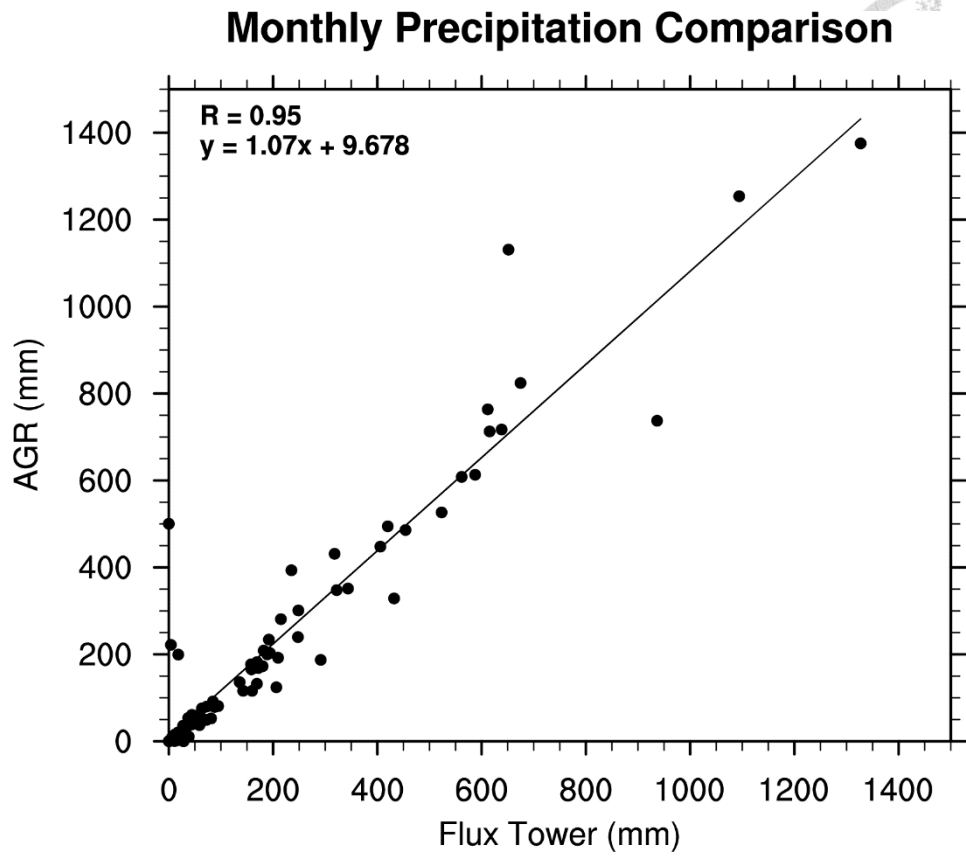


**Figure 3.7** Comparison of LHC monthly rainfall from 2008 to 2016 between flux tower and agricultural station (AGR). The solid line presents linear regression between two datasets, and the p-value < 0.01.

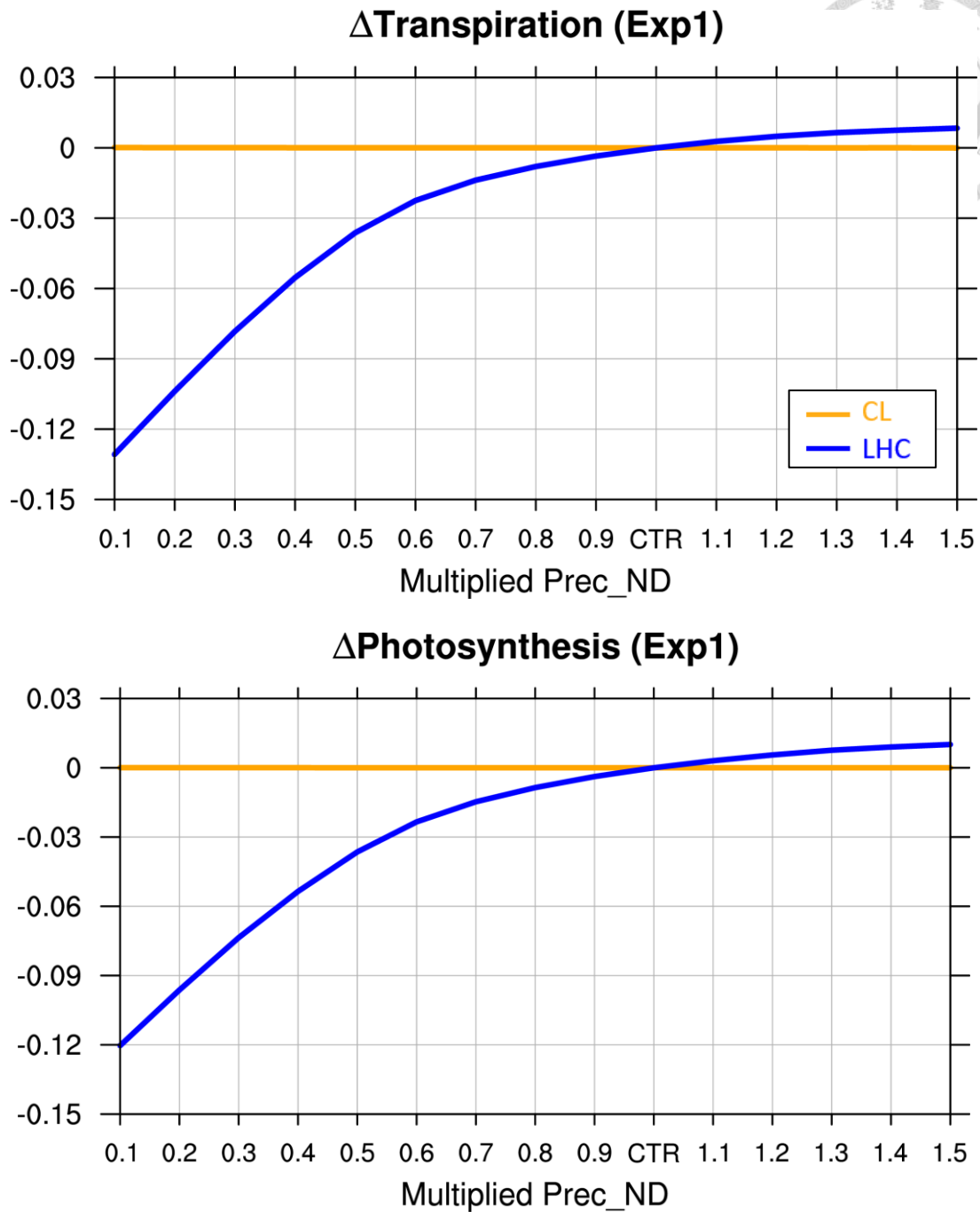


**Figure 3.8** Results of dry season transpiration and photosynthesis from experiment 1. X-axis shows the multiple of Prec\_ND, and Y-axis are the change rate for transpiration and photosynthesis compared to their CTR. (CL: orange line; LHC: blue line)

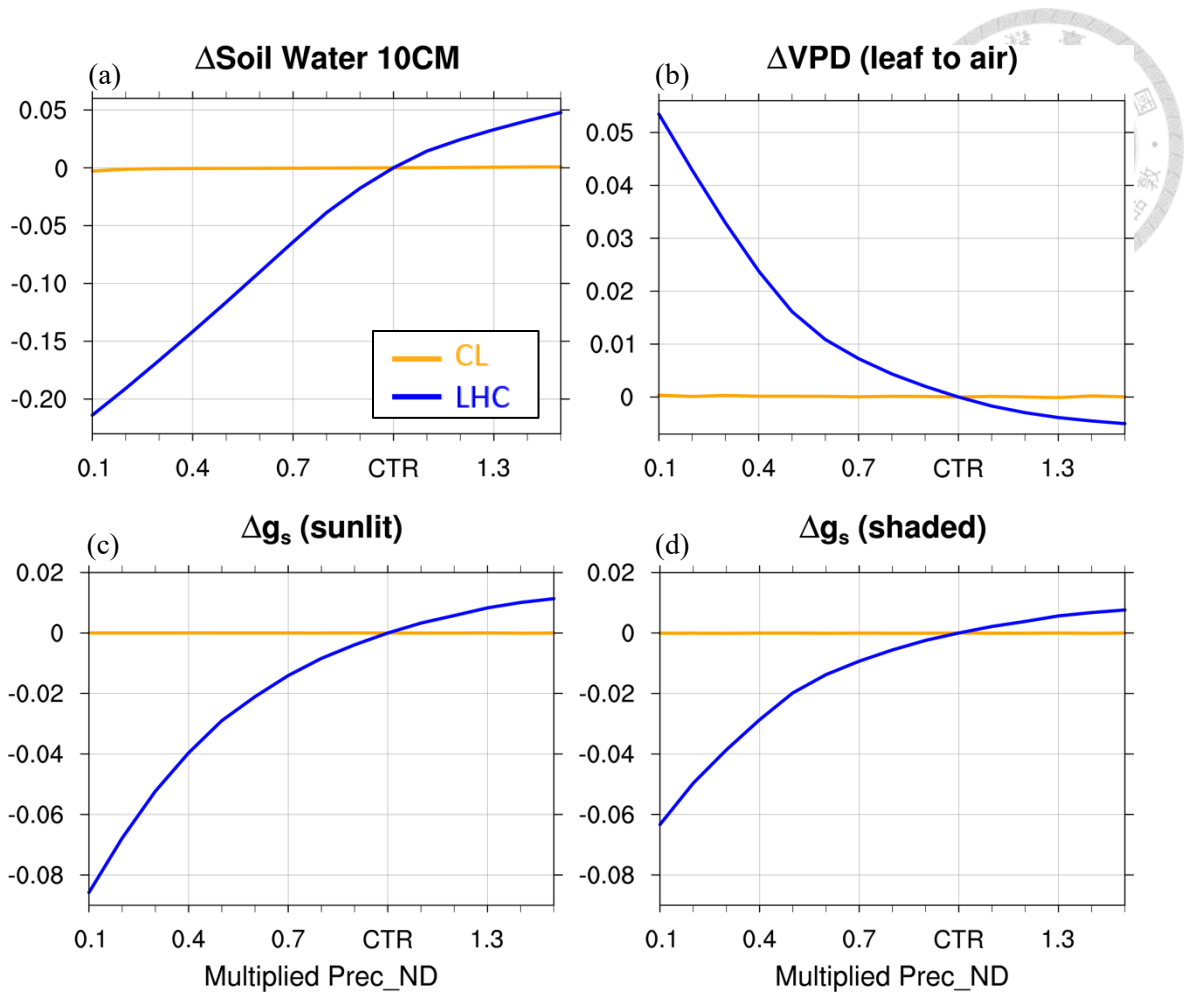


**Figure 3.9** Results of four variables in dry season from from experiment 1. (a) upper 10cm soil water (b) vapor pressure deficit (c) sunlit stomatal conductance (d) shaded stomatal conductance (CL: orange line; LHC: blue line) Y-axis are the change rate for each variable compared to the CTR.

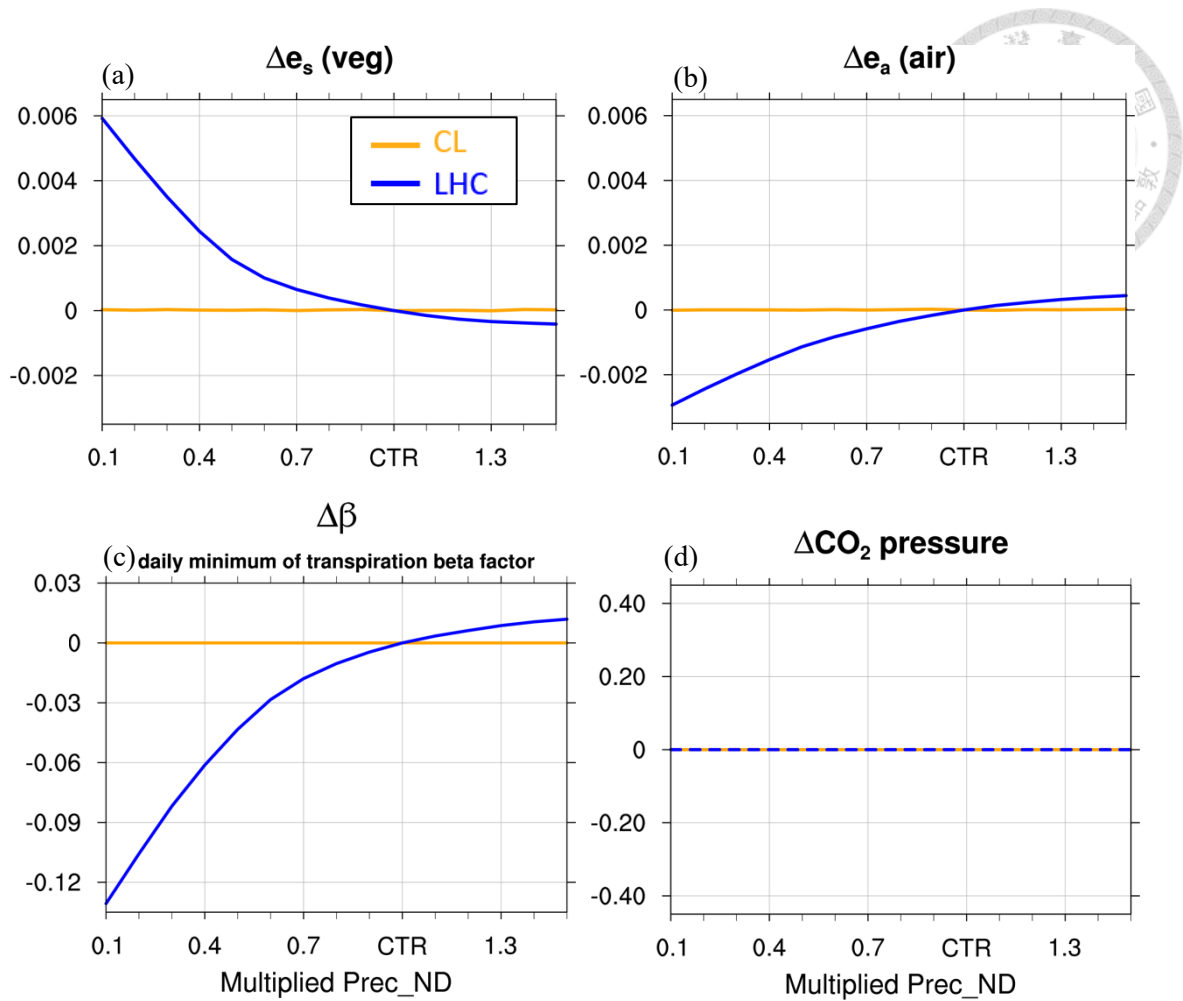


**Figure 3.10** Results of four variables in dry season from experiment 1. (a) saturated vapor pressure (b) air vapor pressure (c) transpiration beta factor (d) CO<sub>2</sub> partial pressure (CL: orange line; LHC: blue line) Y-axes are the change rate for each variable compared to the CTR.

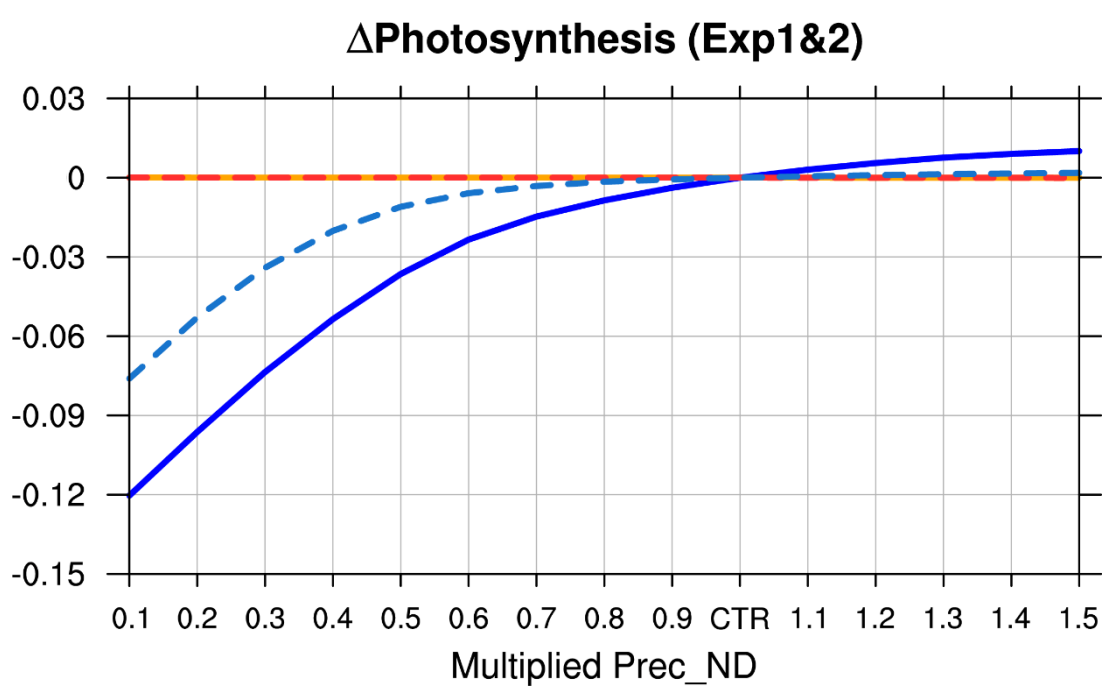
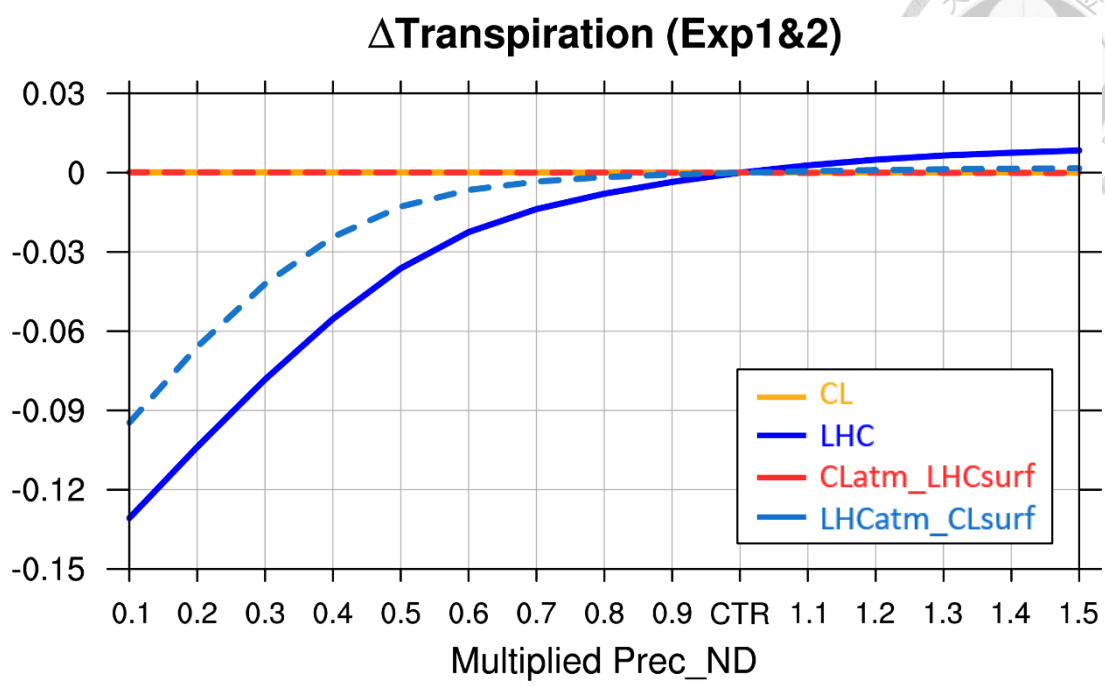
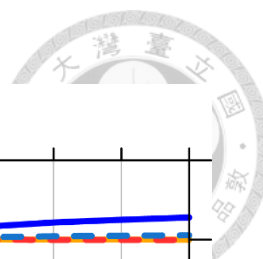


**Figure 3.11** Results of dry season transpiration and photosynthesis from experiment 1 and 2. X-axis shows the multiple of Prec\_ND, and Y-axis are the change rate for transpiration and photosynthesis compared to their CTR. (CL: orange line; LHC: blue line; CLatm\_LHCsurf: red line; LHCatm\_CLsurf: dodgerblue line)



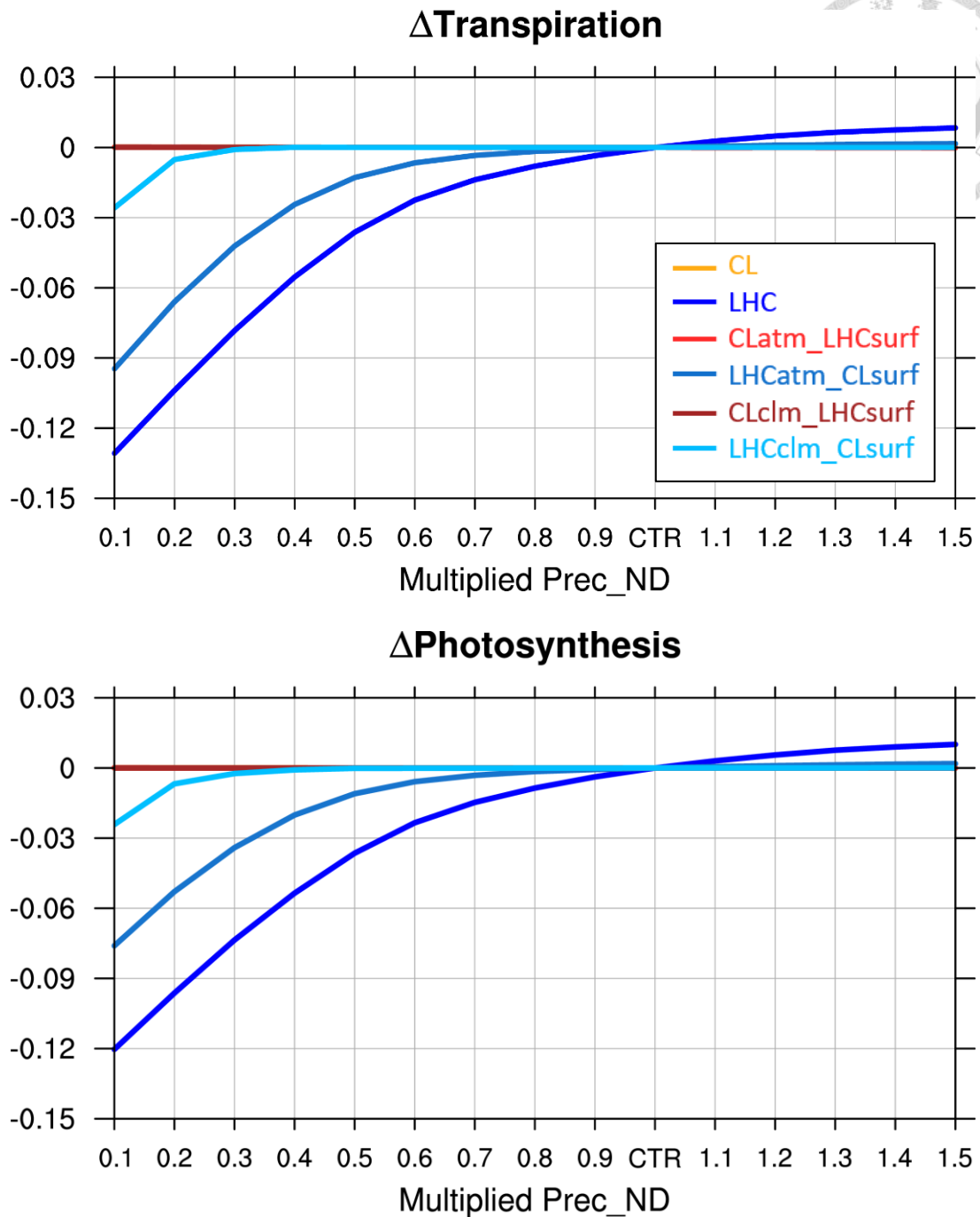


**Figure 3.12** Results of dry season transpiration and photosynthesis from experiment 1 to 3. X-axis shows the multiple of Prec\_ND, and Y-axis are the change rate for transpiration and photosynthesis compared to their CTR. (CL: orange line; LHC: blue line; CLatm\_LHCsurf: red line; LHCatm\_CLsurf: dodgerblue line; CLclm\_LHCsurf: brown line; LHCclm\_CLsurf: lightblue line)

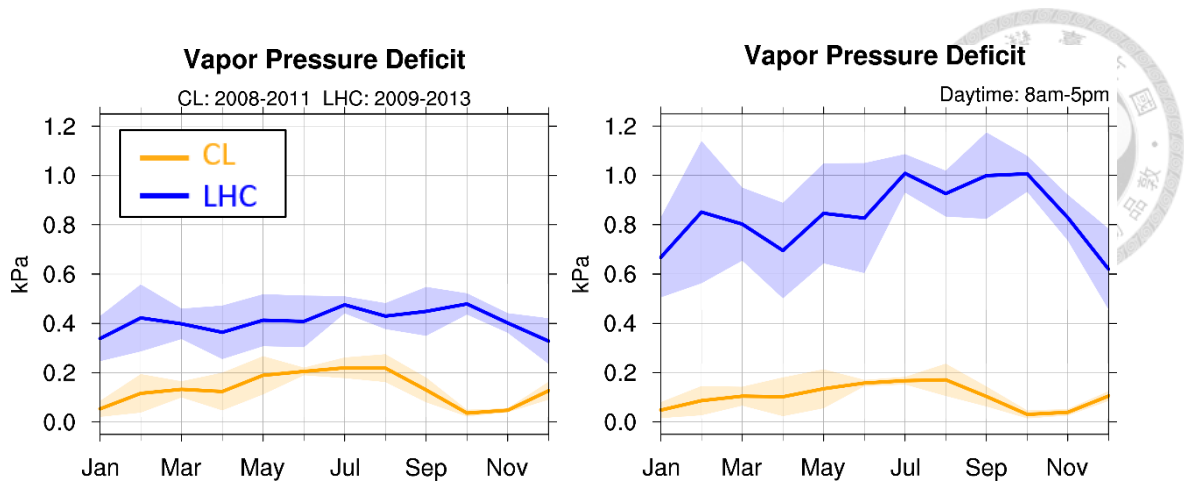


**Figure 3.13** Vapor pressure deficit seasonality calculated by observational flux tower data. Orange line for CL and blue line for LHC. Left picture are the was calculated by total time steps, while right picture only include daytime from 8a.m. to 5p.m. The shading colors represent the variation of VPD between first quartile and third quartile from 4 years in CL and 5 years in LHC.

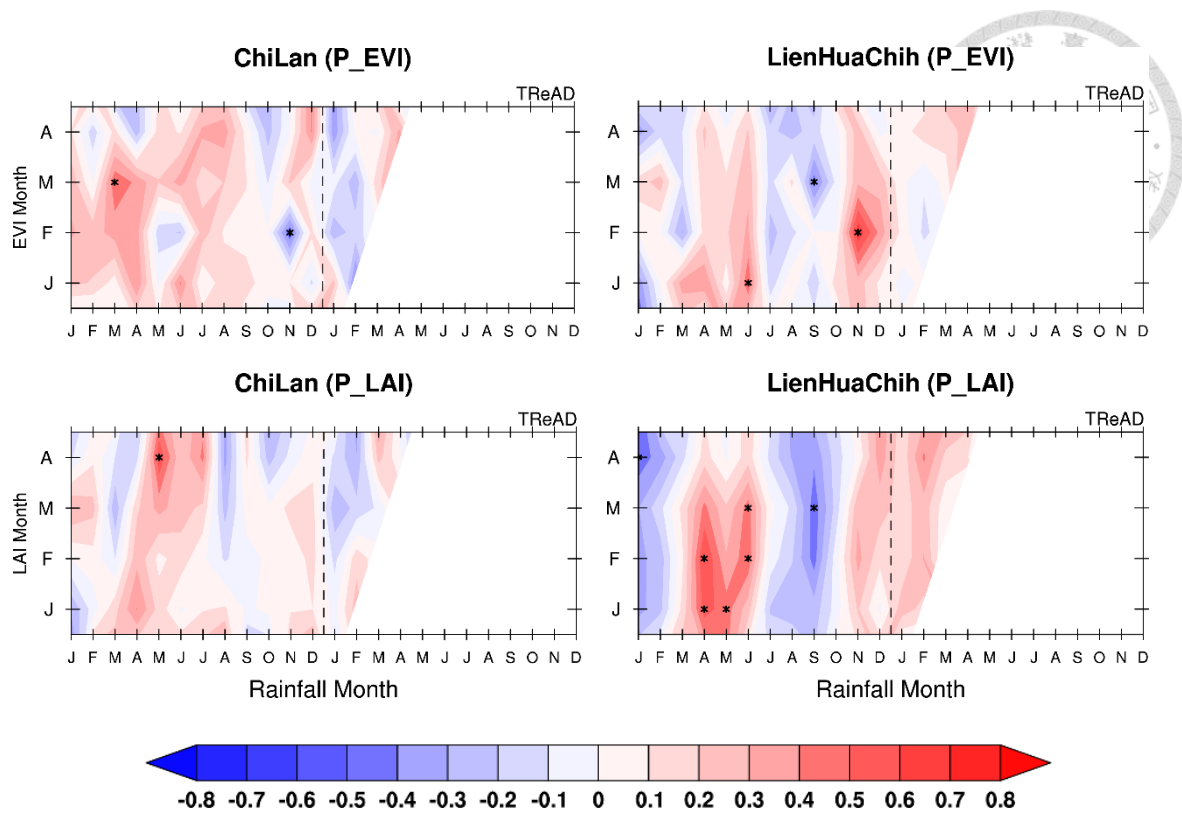


**Figure 4.1** Month to month correlation between TReAD rainfall (P) and EVI (up) and LAI (down) in CL and LHC. To the left of the dashed line present the precipitation in preceding year, while the right present current year. The blank space is vegetation-leading condition, which are not to be considered.

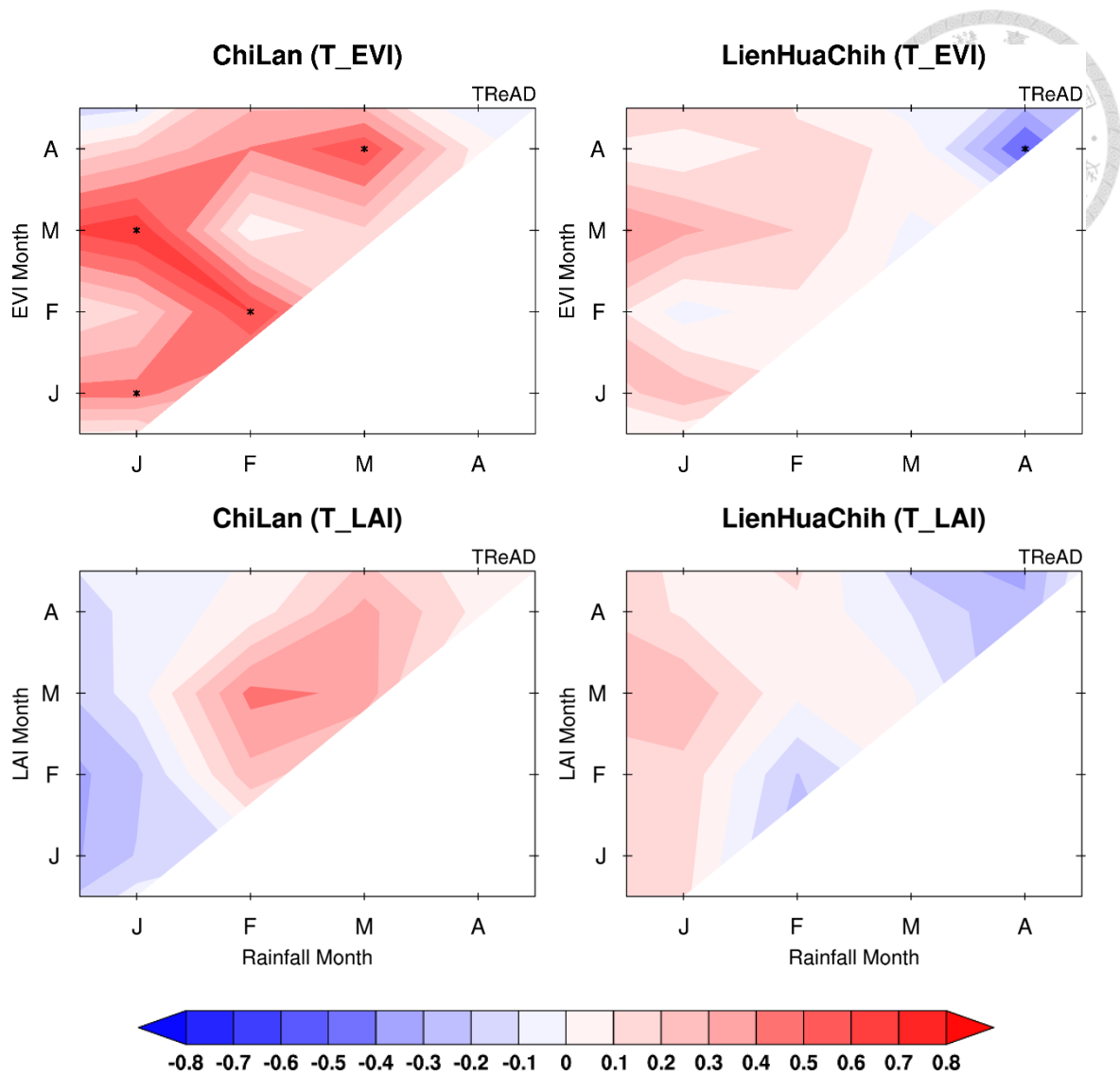


**Figure 4.2** Month to month correlation between TReAD surface temperature (T) and EVI (up) and LAI (down) in CL and LHC. The blank space is vegetation-leading condition, which are not to be considered.

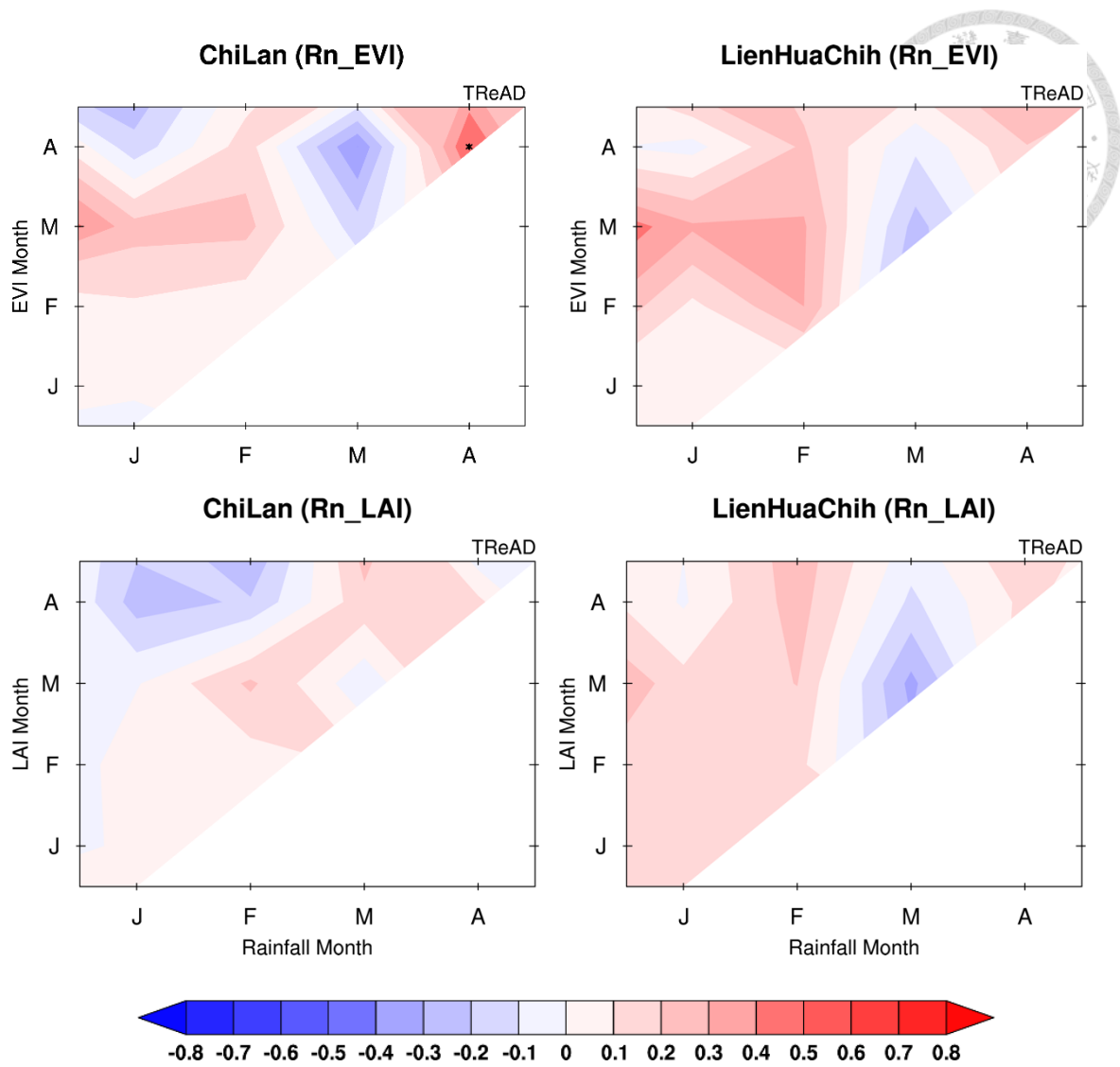


**Figure 4.3** Month to month correlation between TReAD net radiation (Rn) and EVI (up) and LAI (down) in CL and LHC. The blank space is vegetation-leading condition, which are not to be considered.

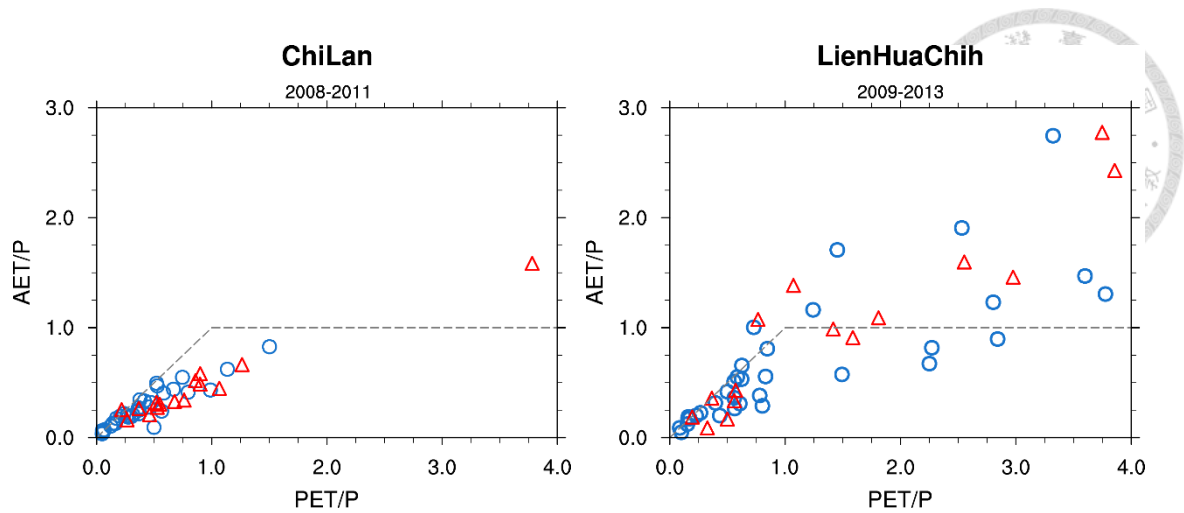


**Figure 4.4** Monthly normalized potential evapotranspiration (PET) and actual evapotranspiration (AET) by precipitation in CL and LHC. Red circles present the calculation from January to April. Dash gray line represent energy and water limited.

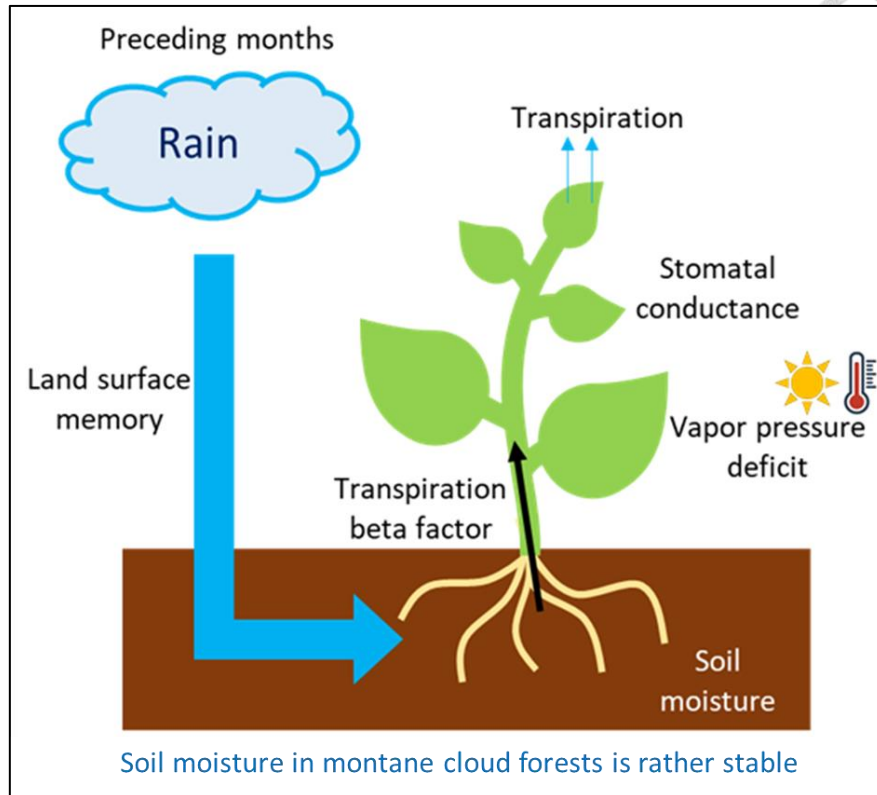


**Figure 5.1** Schematic of low soil water period plant-water relation in tropical non-cloud forests, all the parameters derived from stomatal conductance formula in Community Land Model.

# TABLES

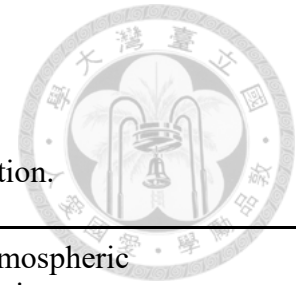


**Table 2.1** Experiment Design in CLM model simulation.

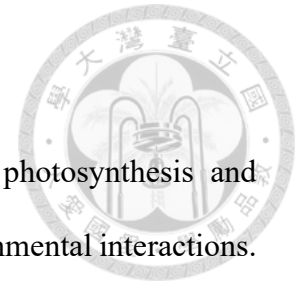
Experiment Number	Name of experiments	Land surface condition	Atmospheric forcing
1	CL	100% evergreen needleleaf tree, annual mean LAI = 4.3, coefficient of maximum allowed dew = 0.2533	CL 2008~2011 half hourly observational data
	LHC	4.64% evergreen needleleaf tree, 57.9% evergreen broadleaf tree, 2.04% deciduous broadleaf tree, 35.22% C3 grass, annual mean LAI = 3.95	LHC 2009~2013 half hourly observational data
2	LHCatm_CLsurf	100% evergreen needleleaf tree, annual mean LAI = 4.3, coefficient of maximum allowed dew = 0.2533	LHC 2009~2013 half hourly observational data
	CLatm_LHCsurf	4.64% evergreen needleleaf tree, 57.9% evergreen broadleaf tree, 2.04% deciduous broadleaf tree, 35.22% C3 grass, annual mean LAI = 3.95	CL 2008~2011 half hourly observational data
3	LHCclm_CLsurf	100% evergreen needleleaf tree, annual mean LAI = 4.3, coefficient of maximum allowed dew = 0.2533	LHC 2009~2011 half hourly observational data <b>Nov. to Dec. Precipitation:</b> CL 2009~2011 half hourly observational rainfall data.
	CLclm_LHCsurf	4.64% evergreen needleleaf tree, 57.9% evergreen broadleaf tree, 2.04% deciduous broadleaf tree, 35.22% C3 grass, annual mean LAI = 3.95	CL 2009~2011 half hourly observational data <b>Nov. to Dec. Precipitation:</b> LHC 2009~2011 half hourly observational rainfall data.



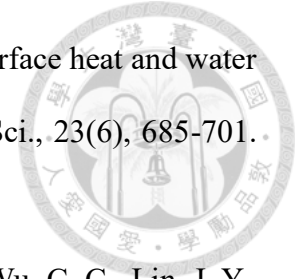
**Table 2.2** Daily average of multiple of November and December precipitation  
(Prec\_ND) in CL and LHC.

<b>Multiple value</b>	<b>CL (mm/day)</b>	<b>LHC (mm/day)</b>
0.1	0.76	0.22
0.2	1.53	0.45
0.3	2.29	0.67
0.4	3.05	0.9
0.5	3.82	1.12
0.6	4.58	1.35
0.7	5.34	1.57
0.8	6.11	1.79
0.9	6.87	2.02
Control Run (CTR)	7.63	2.24
1.1	8.39	2.47
1.2	9.16	2.69
1.3	9.92	2.91
1.4	10.68	3.14
1.5	11.45	3.36

## REFERENCE




- [1] Ainsworth, E. A., & Rogers, A. (2007). The response of photosynthesis and stomatal conductance to rising [CO<sub>2</sub>]: mechanisms and environmental interactions. *Plant Cell and Environment*, 30(2), 258-270. <https://doi.org/10.1111/j.1365-3040.2007.01641.x>
- [2] Allen, R.G., Pereira, L.S., Raes, D., & Smith, M. (1998). Crop evapotranspiration guidelines for computing crop water requirements. FAO Irrigation and Drainage Paper, 56. Rome: United Nations.
- [3] Brown, L., Meier, C., Morris, H., Pastor-Guzman, J., Bai, G., Lerebourg, C., et al. (2020). Evaluation of global leaf area index and fraction of absorbed photosynthetically active radiation products over North America using Copernicus Ground Based Observations for Validation data. *Remote Sensing of Environment*, 247, 111935. <https://doi.org/10.1016/j.rse.2020.111935>
- [4] Bruijnzeel, L. A. (2001). Hydrology of tropical montane cloud forests: a reassessment. *Land Use and Water Resources Research*, 1(1), 1.1-1.18.
- [5] Budyko, M.I. (1974). *Climate and life*. New York, NY: Academic Press.
- [6] Chang, C., Wang, H., & Huang, C. (2017). Assessment of MODIS-derived indices (2001-2013) to drought across Taiwan's forests. *International Journal of Biometeorology*, 62(5), 809-822. <https://doi.org/10.1007/s00484-017-1482-2>
- [7] Chang, S.-C., Lai, I.-L., & Wu, J.-T. (2002). Estimation of fog deposition on epiphytic bryophytes in a subtropical montane forest ecosystem in northeastern Taiwan. *Atmospheric Research*, 64(1-4), 159-167. [https://doi.org/10.1016/S0169-8095\(02\)00088-1](https://doi.org/10.1016/S0169-8095(02)00088-1)
- [8] Chen, Y.-Y., & Li, M.-H. (2012). Determining adequate averaging periods and



reference coordinates for eddy covariance measurements of surface heat and water vapor fluxes over mountainous terrain. *Terr. Atmos. Ocean. Sci.*, 23(6), 685-701. doi: 10.3319/TAO.2012.05.02.01.

- [9] Chu, H. S., Chang, S. C., Klemm, O., Lai, C. W., Lin, Y. Z., Wu, C. C., Lin, J. Y., Jiang, J. Y., Chen, J., & Gottgens, J. F. (2014). Does canopy wetness matter? Evapotranspiration from a subtropical montane cloud forest in Taiwan. *Hydrological Processes*, 28(3), 1190-1214.
- [10] Creed, I., Spargo, A., Jones, J., Buttle, J., Adams, M., Beall, F., et al. (2014). Changing forest water yields in response to climate warming: Results from long-term experimental watershed sites across North America. *Global Change Biology*, 20(10), 3191-3208. doi: 10.1111/gcb.12615
- [11] Dawson, T. E., & Goldsmith, G. R. (2018). The value of wet leaves. *New Phytologist*, 219(4), 1156-1169. <https://doi.org/10.1111/nph.15307>
- [12] Foster, P. (2001). The potential negative impacts of global climate change on tropical montane cloud forests. *Earth-Science Reviews*, 55, 73-106. [https://doi.org/10.1016/S0012-8252\(01\)00056-3](https://doi.org/10.1016/S0012-8252(01)00056-3)
- [13] Foster, P. (2001). The potential negative impacts of global climate change on tropical montane cloud forests. *Earth-Sci. Rev.*, 55, 73-106. [https://doi.org/10.1016/S0012-8252\(01\)00056-3](https://doi.org/10.1016/S0012-8252(01)00056-3)
- [14] Gessner, U., Niklaus, M., Kuenzer, C., & Dech, S. (2013). Intercomparison of Leaf Area Index Products for a Gradient of Sub-Humid to Arid Environments in West Africa. *Remote Sensing*, 5(3), 1235-1257. <https://doi.org/10.3390/rs5031235>
- [15] Gotsch, S., Asbjornsen, H., & Goldsmith, G. (2016). Plant carbon and water fluxes in tropical montane cloud forests. *Journal of Tropical Ecology*, 32 (5), 404-420. doi:10.1017/S0266467416000341

- 
- [16] Gu, R., Lo, M., Liao, C., Jang, Y., Juang, J., Huang, C., Chang, S., Hsieh, C., Chen, Y., Chu, H., & Chang, K. (2021). Early Peak of Latent Heat Fluxes Regulates Diurnal Temperature Range in Montane Cloud Forests. *Journal of Hydrometeorology*, 22(9), 2475-2487.
- [17] Guan, K., Pan, M., Li, H., et al. (2015). Photosynthetic seasonality of global tropical forests constrained by hydroclimate. *Nature Geosci*, 8, 284–289. <https://doi.org/10.1038/ngeo2382>
- [18] Guan, K., Good, S. P., Caylor, K. K., Medvigy, D., Pan, M., Wood, E. F., Sato, H., Biasutti, M., Chen, M., Ahlström, A., & Xu, X. (2018). Simulated sensitivity of African terrestrial ecosystem photosynthesis to rainfall frequency, intensity, and rainy season length. *Environmental Research Letters*, 13(2).
- [19] Huete, A., Didan, K., Miura, T., Rodriguez, E. P., Gao, X., & Ferreira, L. G. (2002). Overview of the radiometric and biophysical performance of the MODIS vegetation indices. *Remote Sensing of Environment*, 83(1-2), 195-213. [https://doi.org/10.1016/S0034-4257\(02\)00096-2](https://doi.org/10.1016/S0034-4257(02)00096-2)
- [20] Klemm, O., Chang, S.-C., & Hsia, Y.-J. (2006). Energy fluxes at a subtropical mountain cloud forest. *Forest Ecology and Management*, 224(1-2), 5-10. <https://doi.org/10.1016/j.foreco.2005.12.003>
- [21] Limm, E., Simonin, K., & Dawson, T. (1970). Foliar uptake of fog in the Coast Redwood Ecosystem: A novel drought-alleviation strategy shared by most redwood forest plants. US Forest Service Research and Development. <https://www.fs.usda.gov/research/treesearch/41148>.
- [22] McAneney, K., & Itier, B. (1996). Operational limits to the Priestley-Taylor formula. *Irrigation Science*, 17(1), 37-43. <https://doi.org/10.1007/s002710050020>.
- [23] Mildenerger, K., Beiderwieden, E., Hsia, Y. J., & Klemm, O. (2009). CO<sub>2</sub> and

water vapor fluxes above a subtropical mountain cloud forest-The effect of light conditions and fog. *Agricultural and Forest Meteorology*, 149 (10), 1730-1736.

- [24] Monteith, J. L. (1965). Evaporation and environment. In *Symposia of the society for experimental biology* (Vol. 19, pp. 205-234). Cambridge University Press (CUP) Cambridge.
- [25] Priestley, C. H. B., & Taylor, R. J. (1972). On the assessment of surface heat flux and evaporation using large scale parameters. *Monthly Weather Review*, 100, 81-92. [http://dx.doi.org/10.1175/1520-0493\(1972\)100<0081:OTAOSH>2.3.CO;2](http://dx.doi.org/10.1175/1520-0493(1972)100<0081:OTAOSH>2.3.CO;2)
- [26] Schulz, H. M., C. F. Li, B. Thies, S. C. Chang, and J. Bendix, 2017: Mapping the montane cloud forest of Taiwan using 12 year MODIS-derived ground fog frequency data. *PLOS ONE*, 12, e0172663, <https://doi.org/10.1371/journal.pone.0172663>.
- [27] Stewart, J. B. (1988). Modelling surface conductance of Pine forest. *Agricultural and Forest Meteorology*, 43, 19-35. [https://doi.org/10.1016/0168-1923\(88\)90003-2](https://doi.org/10.1016/0168-1923(88)90003-2)
- [28] Still, C. J., Foster, P. N., & Schneider, S. H. (1999). Simulating the effects of climate change on tropical montane cloud forests. *Nature*, 398, 608-610. <https://doi.org/10.1038/19293>
- [29] Sepúlveda, M., Bown, H. E., Miranda, M. D., & Fernández, B. (2018). Impact of rainfall frequency and intensity on inter- and intra-annual satellite-derived evi vegetation productivity of an acacia caven shrubland community in central Chile. *SpringerLink*. <https://link.springer.com/article/10.1007/s11258-018-0873-8>
- [30] Tan, Z., Zhao, J., Wang, G., Chen, M., Yang, L., & He, C. et al. (2019). Surface conductance for evapotranspiration of tropical forests: Calculations, variations, and controls. *Agricultural And Forest Meteorology*, 275, 317-328. <https://doi.org/10.1016/j.agrformet.2019.06.006>

- [31] 古鎔與,(2020)。從日變化尺度探討臺灣山區雲霧森林的水文氣候循環及其特殊性。國立臺灣大學理學院大氣科學研究所碩士論文。

